Developmental Biology xxx (2011) xxx–xxx

Contents lists available at SciVerse ScienceDirect

Developmental Biology

journal homepage: www.elsevier.com/developmentalbiology

A dual function of *Drosophila* capping protein on DE-cadherin maintains epithelial integrity and prevents JNK-mediated apoptosis

Barbara Jezowska, Beatriz García Fernández, Ana Rita Amândio, Paulo Duarte, Cláudia Mendes, Catarina Brás-Pereira, Florence Janody *

Instituto Gulbenkian de Ciência, Rua da Quinta Grande 6, P-2780-156 Oeiras, Portugal

ARTICLE INFO

Article history:
Received for publication 19 May 2011
Revised 29 August 2011
Accepted 14 September 2011
Available online xxxx

Keywords:
Capping protein
DE-cadherin
Cell adhesion
JNK-mediated apoptosis
Wingless signalling
Drosophila disc epithelium

ABSTRACT

E-cadherin plays a pivotal role in epithelial cell polarity, cell signalling and tumour suppression. However, how E-cadherin dysfunction promotes tumour progression is poorly understood. Here we show that the actin-capping protein heterodimer, which regulates actin filament polymerization, has a dual function on DE-cadherin in restricted *Drosophila* epithelia. Knocking down capping protein in the distal wing disc epithelium disrupts DE-cadherin and Armadillo localization at adherens junctions and upregulates *DE-cadherin* transcription. In turn, DE-cadherin provides an active signal, which prevents Wingless signalling and promotes JNK-mediated apoptosis. However, when cells are kept alive with the Caspase inhibitor P35, the activity of the JNK pathway and of the Yorkie oncogene trigger massive proliferation of cells that fail to stably retain associations with their neighbours. Moreover, loss of *capping protein* cooperates with the Ras oncogene to induce massive tissue overgrowth. Taken together, our findings argue that in some epithelia, the dual effect of capping protein loss on DE-cadherin triggers the elimination of mutant cells, preventing them from proliferating. However, the appearance of a second mutation that blocks cell death may allow for the development of some epithelial tumours.

Introduction

Epithelial organization is critical for the physiological function of many organs, as it forms a barrier between two environments and permits the polarized absorption and secretion of molecules. Intercellular adhesions between cells are maintained through adherens junctions (AJs). These junctions are highly enriched for E-Cad, which forms cell–cell contacts through homotypic bonds and mediates intracellular connections with the actin cytoskeleton through its interaction with β-catenin (β-Cat) and α-catenin (α-Cat) (Assemat et al., 2008). In addition to their structural function, AJs components also possess signalling capabilities (van Roy and Berx, 2008). β-cat transduces the Wnt/Wingless (Wg) signalling pathway by entering into the nucleus and stimulating transcription (Jamora and Fuchs, 2002), while E-Cad can block proliferation by its ability to sequester the transcriptionally competent pool of β-cat and effectively shut off expression of Lef/TCF/β-cat-responsive genes. Given its ability to down-regulate the canonical Wg pathway and to promote epithelial cell polarity, E-Cad has long been recognized as an important tumour suppressor (Jeanes et al., 2008). Yet, the molecular mechanism by which E-Cad prevents tumour progression is poorly understood.

The *Drosophila* wing disc is a useful model system for the study of signalling pathways and their influence on growth, fate specification, and morphogenesis. The wing imaginal disc forms a single-layered epithelium with a concentrically organized proximal–distal (PD) axis. In the most distal domain is the primordium of the wing blade, surrounded in the proximal domain by the wing hinge primordium, with the notum and pleura at the periphery. In this tissue, the orthologs of the β-cat and E-Cad, respectively Armadillo (Arm) and DE-Cad have also a dual function on cell–cell adhesion and Wg signalling. In the third larval instar, Wg is expressed in a narrow stripe at the dorsal–ventral (D/V) boundary (Baker, 1988), where it activates target genes, including Distal-less (Dll) and Senseless (Sens) (Jafar-Nejad et al., 2006; Neumann and Cohen, 1997; Zecca et al., 1996), and contributes to growth of the distal wing disc mainly by inhibiting c-Jun NH_2-terminal kinase (JNK)-mediated apoptosis (Adachi-Yamada et al., 1999). Overexpression of *DE-cad* in this tissue compromises Wg signalling, while co-expression of *arm* rescues the *DE-cad* overexpression phenotype (Sanson et al., 1996; Widmann and Dahmann, 2009).

In *Drosophila*, activation of JNK encoded by *basket* (*bsk*), activates a variety of target genes, including *misshapen* (*msn*), *puckered* (*puc*) and *Matrix Metalloproteinase 1* (*MMP1*). Following tissue damage or disruption of apical–basal polarity, JNK signalling has been implicated in triggering apoptotic cell death and in stimulating activation of the Hippo (Hpo) pathway transcription co-activator protein Yorkie (Yki) in surviving neighbouring cells. Yki, in turn, induces the regrowth of

* Corresponding author. Fax: +351 21 440 7970.
E-mail address: fjanody@igc.gulbenkian.pt (F. Janody).

0012-1606/$ – see front matter © 2011 Elsevier Inc. All rights reserved.
doi:10.1016/j.ydbio.2011.09.016

damaged tissues through a process referred to as compensatory cell proliferation (Fan and Bergmann, 2008; Perez-Garijo et al., 2009; Ryoo et al., 2004; Sun and Irvine, 2011). By eliminating developmentally aberrant cells from a tissue, JNK signalling has been proposed to ensure developmental robustness, as well as protect organisms against tumour development (Brumby and Richardson, 2003; Igaki et al., 2006; Uhlirova et al., 2005). However, when apoptosis is blocked, cells remain alive ("undead") and JNK signalling can promote cell proliferation (Hariharan and Bilder, 2006; Igaki et al., 2006; McEwen and Peifer, 2005; Ryoo et al., 2004). Moreover, expression of the Ras^{V12} oncogene subverts the pro-apoptotic function of JNK signalling, which becomes a potent inducer of tumour overgrowth and invasion through the expression of MMP1 (Igaki et al., 2006; Leong et al., 2009; Stockinger et al., 2001; Uhlirova and Bohmann, 2006).

Actin filament (F-actin) turnover and organization is a critical regulator of AJs assembly, maintenance, and remodelling (Cavey and Lecuit, 2009). F-actin growth, stability, disassembly and also their organization into functional higher-order networks are controlled by a plethora of actin-binding proteins (ABPs), strongly conserved between species (Winder and Ayscough, 2005). Capping protein (CP), composed of an α (Cpa) and β (Cpb) subunits, acts as a functional heterodimer by restricting accessibility of the filament barbed end, inhibiting addition or loss of actin monomers (Cooper and Sept, 2008). In *Drosophila*, removing either *cpa* or *cpb*, promotes accumulation of F-actin within the cell and gives rise to identical developmental phenotypes (Delalle et al., 2005; Gates et al., 2009; Janody and Treisman, 2006). In the whole larval wing disc epithelium, loss of CP activity reduces Hpo pathway activity and leads to ectopic expression of several Yki target genes that promote cell survival and proliferation (Fernandez et al., 2011; Sansores-Garcia et al., 2011). However, inappropriate growth can only be observed in the proximal wing domain. In the distal wing primordium, *cpa* or *cpb* mutant cells mislocalize the AJs components DE-Cad and Arm, upregulate *puc* expression, extrude and die (Janody and Treisman, 2006). This indicates that while loss of *CP* can under certain conditions result in tissue overgrowth due to inhibition of Hpo pathway activity, other factors such as the polarity status, also determine the survival and growth of the mutant tissue.

Here we investigate the role of the actin-CP heterodimer in survival of cells in the distal wing disc epithelium. We show that CP has a dual function in regulating DE-Cad: it stabilizes DE-Cad at cell–cell junctions, thereby preventing loss of epithelial integrity and inhibits upregulation of the *DE-cad* gene. DE-Cad would otherwise provide an active signal, which affects Wg signalling and promotes JNK-mediated apoptosis. However, when cells lacking *CP* are kept alive, JNK is converted into a potent inducer of proliferation.

Results

Capping protein promotes DE-cadherin and Armadillo localization at adherens junction and prevents cell invasion in the distal wing disc epithelium

Previously, we have shown that while loss of *CP* inhibits Hpo pathway activity in the whole wing disc epithelium, only the proximal wing disc epithelium can overgrow. In the distal wing primordium, *cpa* or *cpb* mutant cells are extruded from the epithelium and undergo apoptosis (Fernandez et al., 2011; Janody and Treisman, 2006). To understand the molecular mechanism by which loss of CP induces apoptosis in this region, we genetically depleted Cpa (*cpa-IR*) or Cpb (*cpb-IR*) by expressing respective double-stranded RNAs under UAS/GAL4 control in defined regions of the distal wing disc epithelium. *hedgehog*-GAL4 (*hh*-GAL4) and *engrailed-GAL4* (en-GAL4) were used to target the posterior compartment, thus allowing comparison to the control wildtype anterior compartment, while *scalloped*-GAL4 (*sd*-Gal4) was used to target the whole distal wing disc epithelium.

Because apoptosis of CP mutant cells could be a secondary consequence of cells losing contact with each other, we analysed the polarity status of tissues with reduced CP levels. Confocal sections of the apical cell surface or perpendicular to the epithelial plane showed that wildtype discs expressing UAS-*mCD8-GFP* under *hh*-Gal4 control displayed homogenous distribution of Arm (Figs. 1A–A′, B–B′) and DE-Cad (Figs. 1C–C′ and D–D′) at AJs, along the anterior–posterior (A/P) axis. In contrast, in the posterior compartment of discs in which Cpa or Cpb were depleted, Arm (Figs. 1E–E′ and F–F′) and DE-Cad (Figs. 1G–G′ and H–H′) levels were reduced at apical sites. We quantified this effect by measuring the ratio of Arm and DE-Cad signals between the posterior and anterior compartments on the apical cell surface of wing disc cells using standard confocal sections. In *hh>GFP* control discs the ratio of Arm and DE-Cad were 1.01 (n = 7) and 0.93 (n = 8) respectively. In contrast, *hh>GFP; cpb-IR* wing imaginal discs displayed a decrease of 31% (ratio: 0.69; $P<0.01$; n = .16) and 28% (0.72; $P<0.001$ n = 15) of Arm and DE-Cad intensity signals respectively at the apical surface of posterior cells. These defects were specific to CP depletion since overexpressing an HA-tagged form of Cpa in *en>cpa-IR* wing discs restored Arm levels at apical sites (compare Figs. S1B–B′ with A–A′). We conclude that in the distal wing disc epithelium, CP localizes DE-Cad and Arm at apical cell junctions.

Arm is a phosphoprotein (Peifer et al., 1994), which migrates on Western blot as a set of proteins of apparent molecular weight of 105–115 kDa (Fig. 1I, lane 1). The slower mobility form of Arm has been proposed to be associated to the membrane, while cytoplasmic Arm might correspond to the faster mobility form (Peifer et al., 1994). If loss of CP triggers the release of Arm from AJs, we expect that, like cells expressing an activated form of Src42A (Shindo et al., 2008), loss of CP would affect the post-translational pools of Arm. As expected, protein extracts expressing UAS-*cpa-IR* under the control of the *daughterless*-Gal4 (*da*-Gal4) ubiquitous driver contained reduced amount of the slower mobility form of Arm ($P<0.003$; n = 5), similar to extracts overexpressing Src64B, used as control (Fig. 1I upper panel, band labelled S). In contrast, in both *da>cpa-IR* and *da>Src64B* the faster mobility form was enriched (Fig. 1I, upper panel, band labelled F). Quantification of the intensity of Arm signals on 5 independent Western blots showed that while knocking down Cpa or overexpressing Src64B always triggered a switch of the slower to the faster mobility forms, the total pool of proteins was not significantly affected. We conclude that CP is required to control the post-translational pools of Arm and in this way may localize Arm at AJs.

Interestingly, many Cpa-depleted cells tended to drop beneath the epithelium, resulting in GFP-expressing cells aberrantly localized basally and recovered into the anterior compartment (white arrows in Figs. 1F and H compared to B and D). To explore the potential role of CP in preventing cellular invasion, we expressed UAS-*cpa-IR*, along with *GFP* to mark the expression domain, under *patched*-GAL4 (*ptc*-GAL4) control that targets a stripe along the A/P compartment boundary. This resulted in Cpa-depleted cells extruding from the normal epithelium and moving away from the *ptc* expression stripe basally (arrows in Figs. S1E–E′ and F–F′). This was never observed in control discs expressing GFP alone (Figs. S1C–C′ and D–D′). Thus, we conclude that CP promotes Arm and DE-Cad localization at AJs, and prevents cell delamination and invasion.

Capping protein maintains DIAP1 levels, prevents activation of JNK signalling and promotes cell survival in the distal wing disc epithelium

Distal wing disc cells lacking CP are eliminated by apoptosis (Janody and Treisman, 2006). We confirmed that knocking down either Cpa, using two independent dsRNA (Figs. 2A–A″ and Figs. S2B–B″), or Cpb (Figs. S2C–C″) triggered the activation of Caspase 3 in numerous cells. These cells were restricted to the distal domain stained by the absence of Hth and localized basally within the distal wing disc epithelium

Please cite this article as: Jezowska, B., et al., A dual function of *Drosophila* capping protein on DE-cadherin maintains epithelial integrity and prevents JNK-mediated apoptosis, Dev. Biol. (2011), doi:10.1016/j.ydbio.2011.09.016

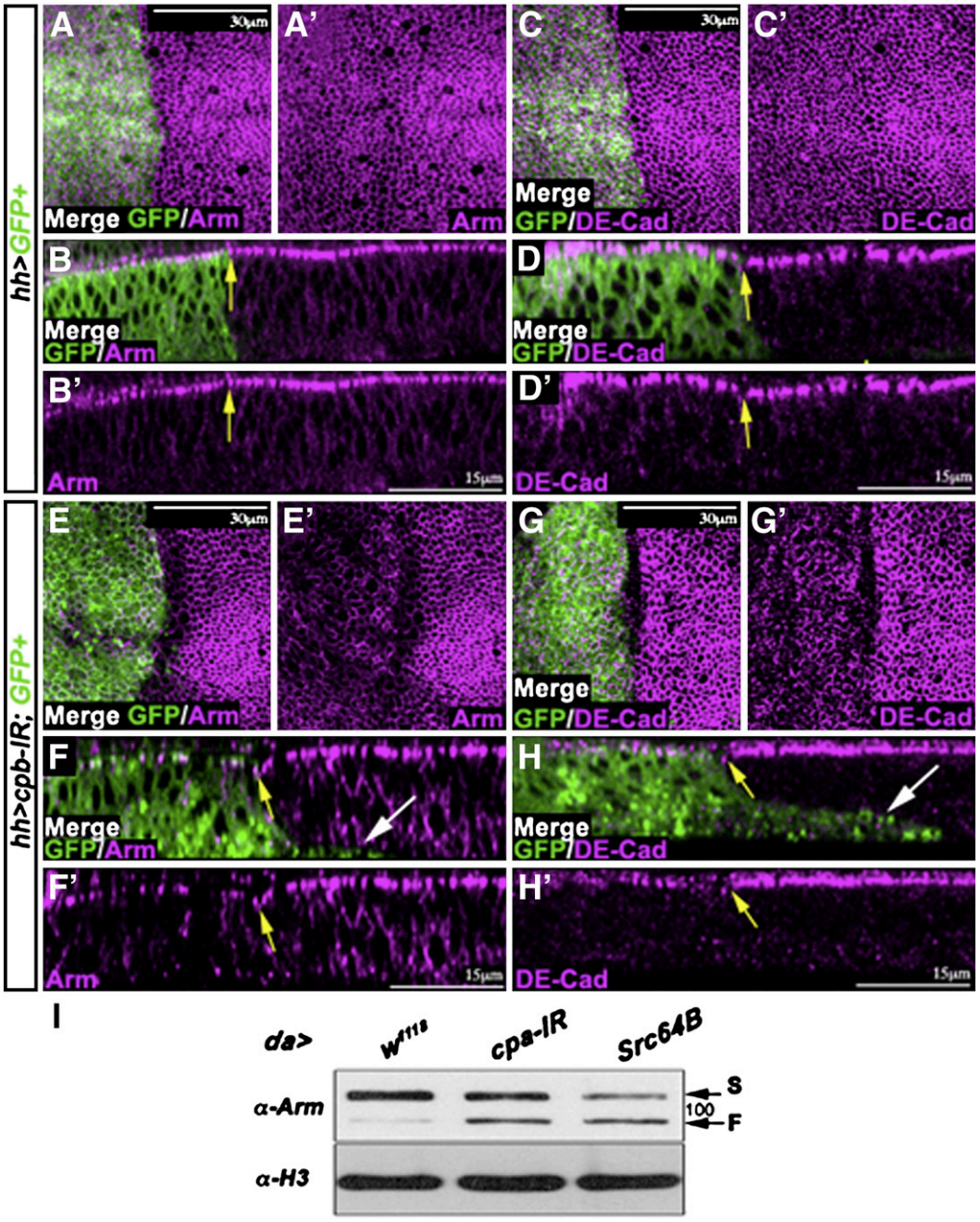

Fig. 1. Loss of CP disrupts the localization of Arm and DE-Cad at AJs and causes cell extrusion and invasion. (A–A′ to H–H′) third instar wing imaginal discs with posterior side to the left. (A–A′, C–C′, E–E′ and G–G′) standard confocal sections of the apical cell surface. (B–B′, D–D′, F–F′ and H–H″) optical cross sections through the distal disc epithelium with apical side up. (A–A′ to D–D′) *hh*-Gal4 driving UAS-*mCD8-GFP* (green in A, B, C and D). (E–E′ to H–H′) *hh*-Gal4 driving UAS-*mCD8-GFP* (green in E, F, G and H) and UAS-*cpb-IR*^{45668}. Discs are stained with (A–A′, B–B′, E–E′ and F–F′) anti-Arm (magenta) or (C–C′, D–D′, G–G′ and H–H′) anti-DE-Cad (magenta). The yellow arrows in B–B′, D–D′, F–F′ and H–H′ indicate the A/P boundaries. The white arrows in F and H indicate Cpa-depleted cells originating from the posterior compartment and moving beneath the anterior compartment. Note that Cpa-depleted cells contains reduced levels of DE-Cad and Arm at the apical cell surface and are recovered beneath the epithelium of the anterior compartment. Scale bars represent 15 or 30 μm as indicated. (I) Western blot on protein extracts from w^{1118} embryos (lane 1) or embryos expressing UAS-*cpa-IR*^{C10} (lane 2) or UAS-*Src64B*^{UY1332} (lane 3) under *da*-Gal4 control, blotted with anti-Arm (upper panel) and anti-H3 (lower panel). S and F indicate the slower and faster mobility forms respectively. Note that in Cpa-depleted tissues, the amount of the slower mobility form of Arm is reduced, while the faster mobility form is enriched.

(Figs. 2A–A″). Expressing *cpa-IR* and *GFP* in the posterior compartment with *hh*-Gal4 showed that all cells stained for activated Caspase 3 were also positive for GFP (Figs. 2B–B″), indicating cell-autonomous apoptosis. Most extruding Cpa-depleted cells moving to areas distant from the *hh* domain expressed activated Caspase 3 (blue arrows in Figs. 2B–B″), showing that invading cells undergo cell death. Apoptosis was due to Cpa loss since expressing an HA-tagged form of Cpa fully suppressed death of cells knocked down for Cpa (Fig. S2 compare E–E″ with D–D″). We then investigated the mechanism by which CP prevents apoptosis. *Drosophila* Inhibitor of Apoptosis 1 (DIAP1) is ubiquitously expressed in imaginal discs (Yoo et al., 2002) and essential to prevent inappropriate caspase activation and apoptosis (Goyal et al., 2000; Ryoo et al., 2004; Wang et al., 1999). In contrast to *hh>GFP* control discs (Figs. 2C–C″), DIAP1 protein was strongly reduced cell-autonomously in tissues expressing *cpa-IR* and GFP under *hh*-Gal4 control (Figs. 2D–D″). To confirm that CP affects DIAP1 levels, we analysed cells mutant for a loss of function allele of *cpa*. To induce mutant cells, in a manner that permits the recovery of cells within the distal wing epithelia at the end of third instar, we used

Please cite this article as: Jezowska, B., et al., A dual function of *Drosophila* capping protein on DE-cadherin maintains epithelial integrity and prevents JNK-mediated apoptosis, Dev. Biol. (2011), doi:10.1016/j.ydbio.2011.09.016

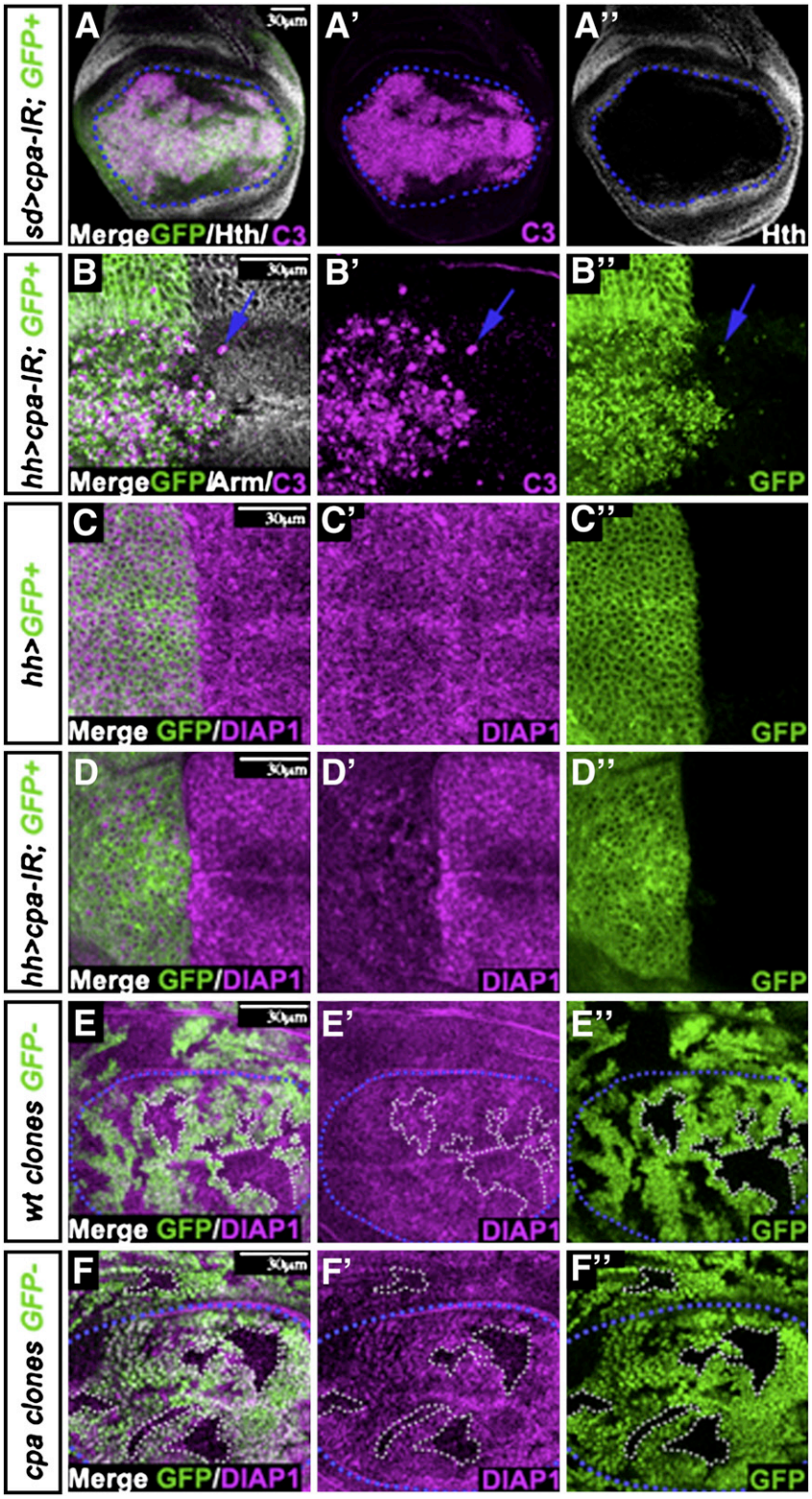

Fig. 2. Loss of CP induces massive cell death in the distal wing disc epithelium and downregulates DIAP1 protein levels. All panels show standard confocal sections of third instar wing imaginal discs with posterior side to the left and dorsal side up. (A–A″) *sd*-Gal4 driving UAS-*mCD8-GFP* (green in A) and UAS *cpa-IR*^{C10}. The disc is stained with anti-C3 (magenta in A and A′) and anti-Hth (white in A and A″). (B–B″) *hh*-Gal4 driving UAS-*mCD8-GFP* (green in B and B″) and UAS *cpa-IR*^{C10}. The disc is stained with anti-C3 (magenta in B and B′) and anti-Arm (white in B). The blue arrows in B, B′ and B″ indicate cells expressing activated C3 and GFP. (C–C″ and D–D″) *hh*-Gal4 driving UAS-*mCD8-GFP* (green in C, C″, D and D″) and (D–D″) UAS *cpa-IR*^{C10}. Discs are stained with anti-DIAP1 (magenta in C, C′, D and D′). (E–E″ and F–F″) *T155*-Gal4; UAS-*flp*-induced (E–E″) FRT42D wildtype or (F–F″) FRT42D *cpa*^{107E} clones marked by the absence of GFP (green in E, E″, F and F″). Discs are stained with anti-DIAP1 (magenta in E, E′, F and F′). The blue dashed lines outline the distal wing domain. The white dashed lines outline *cpa* mutant clones. Scale bars represent 30 μm.

the epithelial-specific Gal4 driver (*T155*-Gal4), which directs expression of the *flipase* (UAS-*flp*) at all larval stages (see Materials and methods). A cell-autonomous decrease in DIAP1 protein levels was also observed in all patches of *cpa* mutant cells that remained in the distal wing disc epithelium (Figs. 2F–F″), whereas wildtype control patches showed normal levels of DIAP1 (Figs. 2E–E″).

Please cite this article as: Jezowska, B., et al., A dual function of *Drosophila* capping protein on DE-cadherin maintains epithelial integrity and prevents JNK-mediated apoptosis, Dev. Biol. (2011), doi:10.1016/j.ydbio.2011.09.016

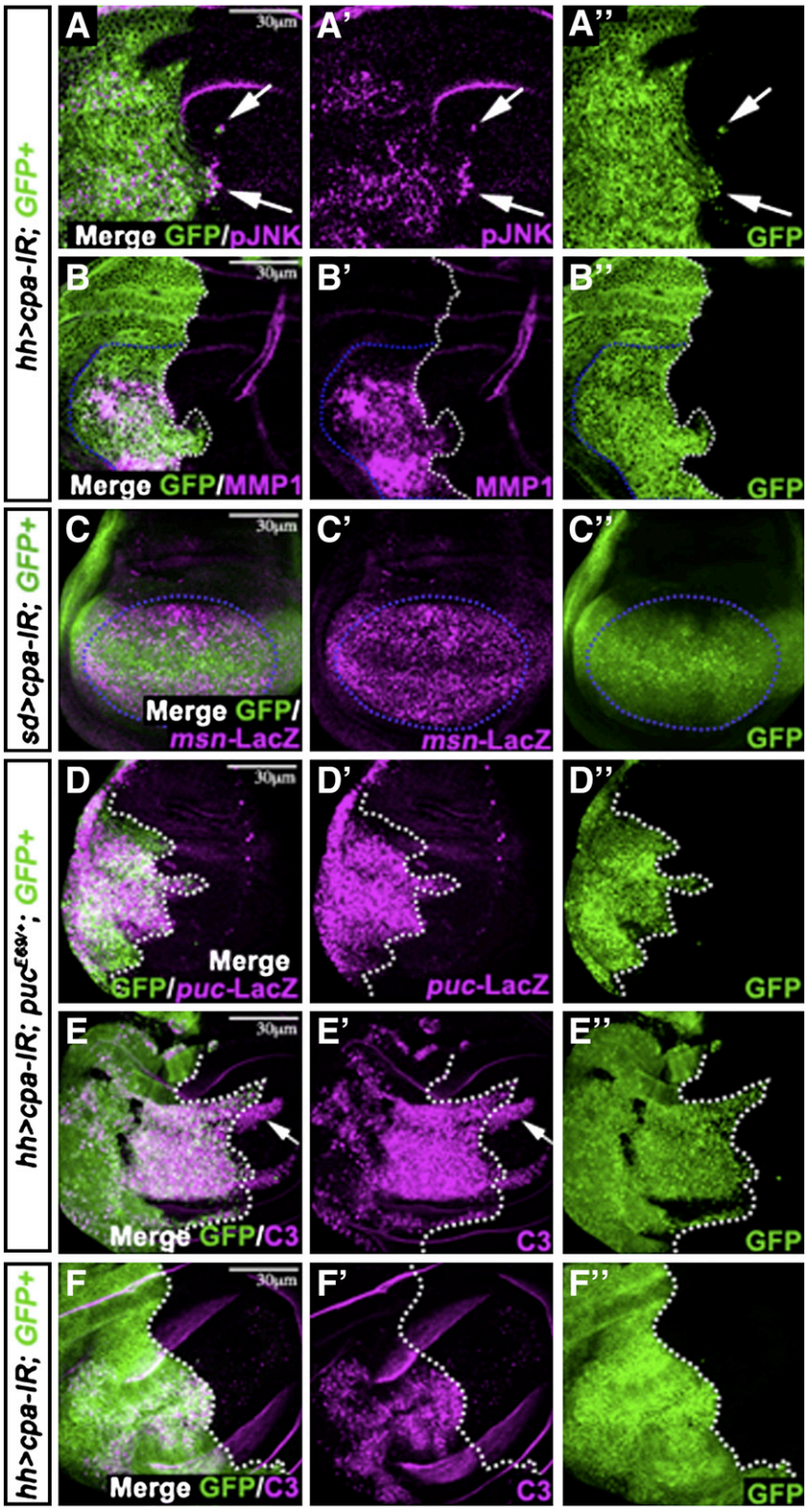

Fig. 3. Loss of CP activates JNK signalling. All panels show standard confocal sections of third instar wing imaginal discs with posterior side to the left and dorsal side up. (A–A″ and B–B″) *hh*-Gal4 driving UAS-*mCD8-GFP* (green in A, A″, B and B″) and UAS *cpa-IR*^{C10}. Discs are stained with (A–A″) anti-pJNK (magenta in A and A′) or (B–B′) anti-MMP1 (magenta in B and B′). The white arrows in A–A″ indicate cells that are stained for both GFP and pJNK. (C–C″) discs carrying a *LacZ* insertion into the *msn* (*msn*^{06946}) locus, expressing UAS-*mCD8-GFP* (green in C and C″) and UAS-*cpa-IR*^{C10} under *sd*-Gal4 control and stained with anti-β-galactosidase (magenta in C and C′) to reveal *msn*-LacZ. (D–D″ and E–E″) discs carrying a *LacZ* insertion into the *puc* (*puc*^{E69}) locus, expressing UAS-*mCD8-GFP* (green in D, D″, E and E″) and UAS-*cpa-IR*^{C10} under *hh*-Gal4 control and stained with (D–D″) anti-β-galactosidase (magenta in D and D′) to reveal *puc*-LacZ or (E-E″) anti-C3 (magenta in E and E′). The white arrows in E and E′ indicate cells that are stained for anti-C3 but are not expressing GFP. (F–F″) *hh*-Gal4 driving UAS-*mCD8-GFP* (green in F and F″) and UAS *cpa-IR*^{C10}. The disc is stained with anti-C3 (magenta in F and F′). The blue dashed lines in B–B″ and C–C″ outline the distal wing disc domain. The white dashed lines in B–B″, D–D″, E–E″ and F–F″ outline the border between the posterior cells expressing *GFP* and *cpa-IR* and the anterior wildtype cells. Scale bars represent 30 μm.

Please cite this article as: Jezowska, B., et al., A dual function of *Drosophila* capping protein on DE-cadherin maintains epithelial integrity and prevents JNK-mediated apoptosis, Dev. Biol. (2011), doi:10.1016/j.ydbio.2011.09.016

Because activation of the JNK signalling pathway can occur in response to DIAP1 inactivation (Kuranaga et al., 2002; Ryoo et al., 2004) and has been implicated in activating the cell death machinery (Igaki, 2009), we next analysed the consequence of knocking down CP on JNK signalling. Cells expressing *cpa-IR* and *GFP* under *hh*-Gal4 control displayed cell-autonomous activation of Bsk, as seen by ectopic staining of phosphorylated JNK in the *hh* domain and in cells moving to distant areas (arrows in Figs. 3A–A″). Moreover, MMP1 (Figs. 3B–B″) and the two reporters of JNK signalling, the *LacZ* enhancer trap insertions in the *msn* (*msn-LacZ*) (Figs. 3C–C″) and *puc* (*puc-lacZ)* (Figs. 3D–D″) genes were also ectopically expressed in Cpa-depleted tissues marked with GFP. Activation of JNK signalling may result from reduced DIAP1 levels, since overexpressing *DIAP1* in tissues in which Cpa expression has been knocked down strongly reduced apoptosis (Fig. S3 compare B with A) and MMP1 upregulation (Figs. S3C–C′ and compare B′ with A′) but did not prevent F-actin accumulation (Figs. S3D–D′). Taken together, we conclude that CP is required to maintain DIAP1 levels, prevents activation of JNK signalling and promotes cell survival in the distal wing disc epithelium.

JNK signalling triggers apoptosis but not polarity loss of capping protein-depleted cells

We noticed that the *puc*-LacZ reporter, which is also a *puc* allele, enhanced the death of *hh>cpa-IR*-depleted tissues (Fig. 3 compare E–E″ with F–F″). Although some apoptotic cells did not express GFP (arrow in Figs. 3E–E′), these cells are unlikely to die non-autonomously since they were recovered in patches away from the *hh*-Gal4-expressing domain. Instead, these cells may have lost their differentiation state and fail to express the *hh*-Gal4 driver. Because Puc is a negative regulator of JNK, activation of JNK signalling might be sufficient to trigger apoptosis of cells lacking CP. If so, decreasing JNK signalling by expressing a dominant-negative form of *bsk* (bsk^{DN}) should suppress death in cells with reduced Cpa. Expressing bsk^{DN} with *sd*-Gal4 did not induce morphological aberrations (Figs. 4A–A″), nor did it significantly alter the apical F-actin network (Fig. 4B), but it abolished apoptosis and ectopic MMP1 expression of tissues expressing UAS-$cpa\text{-}IR^{C10}$ (Fig. 4 compare I–I″ with E–E″) or UAS-$cpa\text{-}IR^{100773}$ (data not shown). However, F-actin accumulation was still observed in the distal domain of wing imaginal disc expressing both, *cpa-IR* and bsk^{DN} (Fig. 4J), similar to tissues expressing *cpa-IR* and *GFP* (Fig. 4F). We conclude that Cpa-depleted cells die via JNK-mediated apoptosis.

We then asked if altered polarity of Cpa-depleted tissues was also dependent upon JNK activation. To identify cells basally localized that may have been extruded from the disc epithelium, we analysed optical cross sections through distal wing disc epithelia, stained with the TOTO3 nuclear dye and Phalloidin to outline the cell membrane. As expected, Cpa-depleted tissues showed basally extruded pycnotic nuclei located below the epithelium proper (yellow arrow in Fig. 4G) that were stained for activated Caspase 3 (Figs. S4E–E′). Distal wing disc epithelia expressing both *cpa-IR* and bsk^{DN} also displayed basally extruded nuclei surrounded by dense F-actin patches that did not appear pycnotic (yellow arrows in Figs. 4K–K′). This was never observed in discs expressing bsk^{DN} alone (Figs. 4C–C′). Strikingly, Cpa-depleted tissues expressing bsk^{DN} also displayed many ectopic staining for the marker of mitotic chromatin, phospho-Histone 3 (pH3), on the basal surface of the distal wing disc epithelium (11 to 26 mitotic figures per disc; n = 15) (Figs. 4L–L′ and Figs. S4F–F″, G–G″). In contrast, tissues expressing bsk^{DN} (Figs. 4D–D′ and Figs. S4A–A″, B–B″) or *cpa-IR* (Figs. 4H–H′ and Figs. S4C–C″, D–D″) alone with GFP showed mitotic figures almost exclusively at the apical cell surface (1 mitotic figure on the basal cell surface per disc; n = 20). This defect indicates that loss of CP affects cell polarity independently of JNK activation. CP might be required for the proper polarization of the mitotic spindles or for maintaining a polarized epithelial organization. Taken together, we conclude that in cells lacking CP, apoptosis is JNK-dependent, while the polarity defects and excess F-actin are JNK-independent.

DE-cadherin promotes JNK-mediated apoptosis of capping protein-depleted cells

Alternatively, loss of adhesive strength between cells might trigger JNK-mediated apoptosis (Igaki et al., 2006). If so, reducing DE-Cad levels in Cpa-depleted cells would be expected to further enhance the decrease of DE-Cad adhesion. Heterozygote mutant tissues for *DE-cad* that expressed *GFP* under *hh*-Gal4 control did not show visible defects (Figs. 5A–A′ to D–D′). Surprisingly, Caspase 3 activation was 26% reduced ($P<0.002$; n = 20) when one copy of *DE-cad* was removed in *hh>cpa-IR* wing imaginal discs (Fig. 5 compare I–I′ with E–E′). Moreover, reducing *DE-cad* levels in cells knocked down for Cpa, partially suppressed MMP1 upregulation (Fig. 5 compare J–J′ with F–F′). Apoptosis of Cpb-depleted tissues (*sd>*$cpb\text{-}IR^{45668}$) was also partially rescued when one copy of the cad^2 mutant allele was removed (data not shown). However, reducing DE-Cad levels in *hh>cpa-IR* wing discs did not restore the intensity signals of Arm at the apical cell surface (Fig. 5 compare K–K′ to G–G′; 28% reduction in *hh>cpa-IR; DE-Cad*$^{+/-}$; n = 15 versus 31% in *hh>cpa-IR; DE-Cad*$^{+/+}$; n = 11), nor prevented F-actin accumulation (Fig. 5 compare L–L′ with H–H′). Therefore, in Cpa-depleted tissues, DE-Cad may be part of a signalling network that triggers JNK-mediated cell death.

Capping protein downregulates DE-cadherin expression

To understand the role of DE-Cad in promoting apoptosis of cells knocked down for CP, we tested if CP regulates the levels of DE-Cad. As previously described (Jaiswal et al., 2006), in control *hh>GFP* wing imaginal disc, a *lacZ* enhancer trap insertion in the *shotgun* gene (*shg*-LacZ), which encodes for *DE-cad*, showed high levels of expression in cells flanking the D/V boundary (Figs. 6A–A″) and in posterior cells apposed to the A/P boundary (arrow in Figs. 6A–A′). Interestingly, *shg*-LacZ was upregulated cell autonomously in *hh>cpa-IR* depleted tissues (Figs. 6B–B″). When we analysed mutant clones for the cpb^{M143} allele, we noticed that transcriptional upregulation of *shg*-LacZ was observed in extruded mutant cells located in the distal wing disc domain (white arrows in Figs. 6C–C″ and magnification in D–D″) but also in all clones that maintained a polarized epithelial architecture in the proximal wing region (yellow arrows in Figs. 6C–C″). We then analysed by Western blot the amount of DE-Cad in protein extracts from first instar larvae expressing either *GFP* or *cpa-IR* or Src64B. As previously reported for Src42A overexpression (Shindo et al., 2008), the levels of DE-Cad protein were reduced by 50 to 80% ($P<0.005$; n = 3) in tissues overexpressing Src64B. In contrast, extracts expressing *cpa-IR* contained 2 to 4 folds ($P<.0.02$; n = 4) increase of DE-Cad levels compared to *da>GFP* control extracts (Fig. 6E, upper panel). Taken together, we conclude that in cells lacking CP, *DE-cad* transcription is upregulated and correlates with increase DE-Cad levels. However, DE-Cad is unable to localize properly at AJs.

DE-cadherin prevents Wingless signalling of cells knocked down for capping protein

We then asked how DE-Cad triggers JNK-mediated cell death. Over-expression of *Drosophila DE-cad* can sequester Arm and prevent it from participating in Wg signalling (Sanson et al., 1996; Widmann and Dahmann, 2009). Since, decreased Wg signalling promotes JNK-dependent apoptosis in the distal wing disc epithelium (Adachi-Yamada et al., 1999), DE-Cad may trigger JNK-mediated apoptosis of Cpa-depleted cells, by sequestering Arm. If so, we would expect that Wg signalling is affected in cells lacking CP. Indeed, while Wg (Figs. 7A–A′) and *wg*-LacZ (Figs. 7B–B′) were still present at the

Please cite this article as: Jezowska, B., et al., A dual function of *Drosophila* capping protein on DE-cadherin maintains epithelial integrity and prevents JNK-mediated apoptosis, Dev. Biol. (2011), doi:10.1016/j.ydbio.2011.09.016

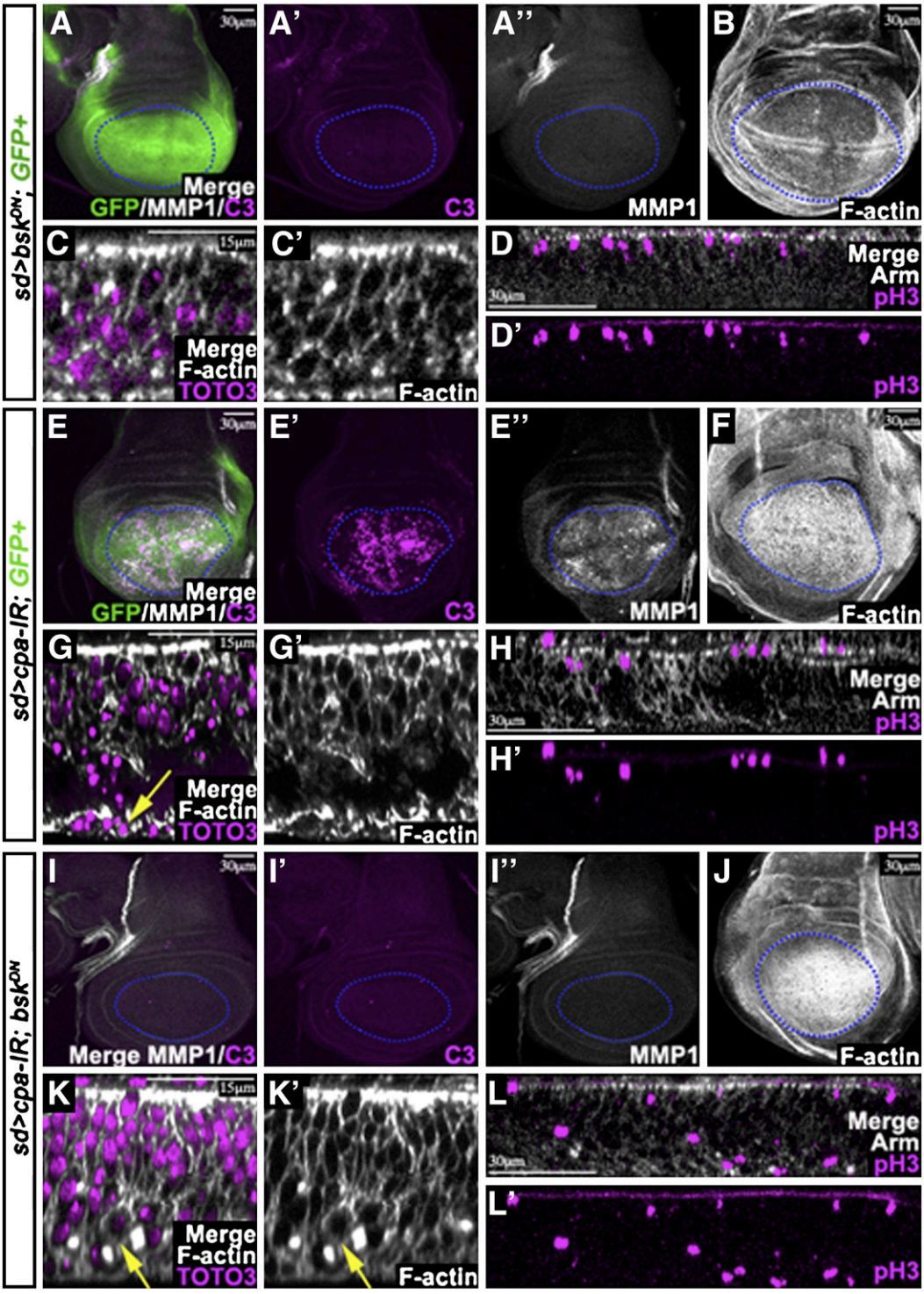

Fig. 4. Expressing bsk^{DN} in Cpa-depleted cells prevents apoptosis but does not suppress excess F-actin nor the polarity defects. All panels show third instar wing imaginal discs. (A–A″, B, E–E″, F, I–I″ and J) standard confocal sections with posterior side to the left and dorsal side up. (C–C′ D–D′, G–G′, H–H′, K–K′ and L–L′) optical cross sections through the distal disc epithelium with apical side up. *sd*-Gal4 driving (A–A″ to D–D′) UAS-bsk^{DN} and UAS-*mCD8-GFP* (green in A) or (E–E″ to H–H′) UAS-*cpa-IR*^{C10} and UAS-*mCD8-GFP* (green in E) or (I–I″ to L–L′) UAS-*cpa-IR*^{C10} and UAS-bsk^{DN}. Discs are stained with (A–A″, E–E″ and I–I″) anti-C3 (magenta in A, A′, E, E′, I and I′) and anti-MMP1 (white in A, A″, E, E″, I and I″) or (B, C–C′, F, G–G′, J and K–K′) Phalloidin to mark F-actin (white) and (C–C′, G–G′ and K–K′) TOTO3 (magenta in C, G and K) to mark the cell nuclei or (D–D′, H–H′ and L–L′) anti-Arm (white in D, H and L) and anti-pH3 (magenta). The blue dashed lines in A–A″, B, E–E″, F, I–I″ and J outline the distal wing disc domain. The yellow arrows in G, K and K′ indicate basally extruded cells. Scale bars represent 15 or 30 μm as indicated.

D/V boundary of posterior cells expressing *cpa-IR* and *GFP*, Sens (Figs. 7C–C′) and Dll (Figs. 7D–D′) expressions were strongly reduced, arguing that CP is required for the expression of Wg-dependent genes. We then analysed the role of DE-Cad in CP-dependent Wg signalling. *hh>GFP* control wing discs that were heterozygote mutant for *DE-cad* expressed Sens (Figs. 7E–E′) and Dll (Figs. 7F–F′) at the D/V boundary. Interestingly, removing one copy of *DE-cad* partially restored the loss of Sens (arrows in Figs. 7G–G′) and Dll (arrows in Figs. 7H–H′) expression due to Cpa depletion. We quantified this effect by measuring the ratio of Sens intensity signals between the posterior and anterior wing

Please cite this article as: Jezowska, B., et al., A dual function of *Drosophila* capping protein on DE-cadherin maintains epithelial integrity and prevents JNK-mediated apoptosis, Dev. Biol. (2011), doi:10.1016/j.ydbio.2011.09.016

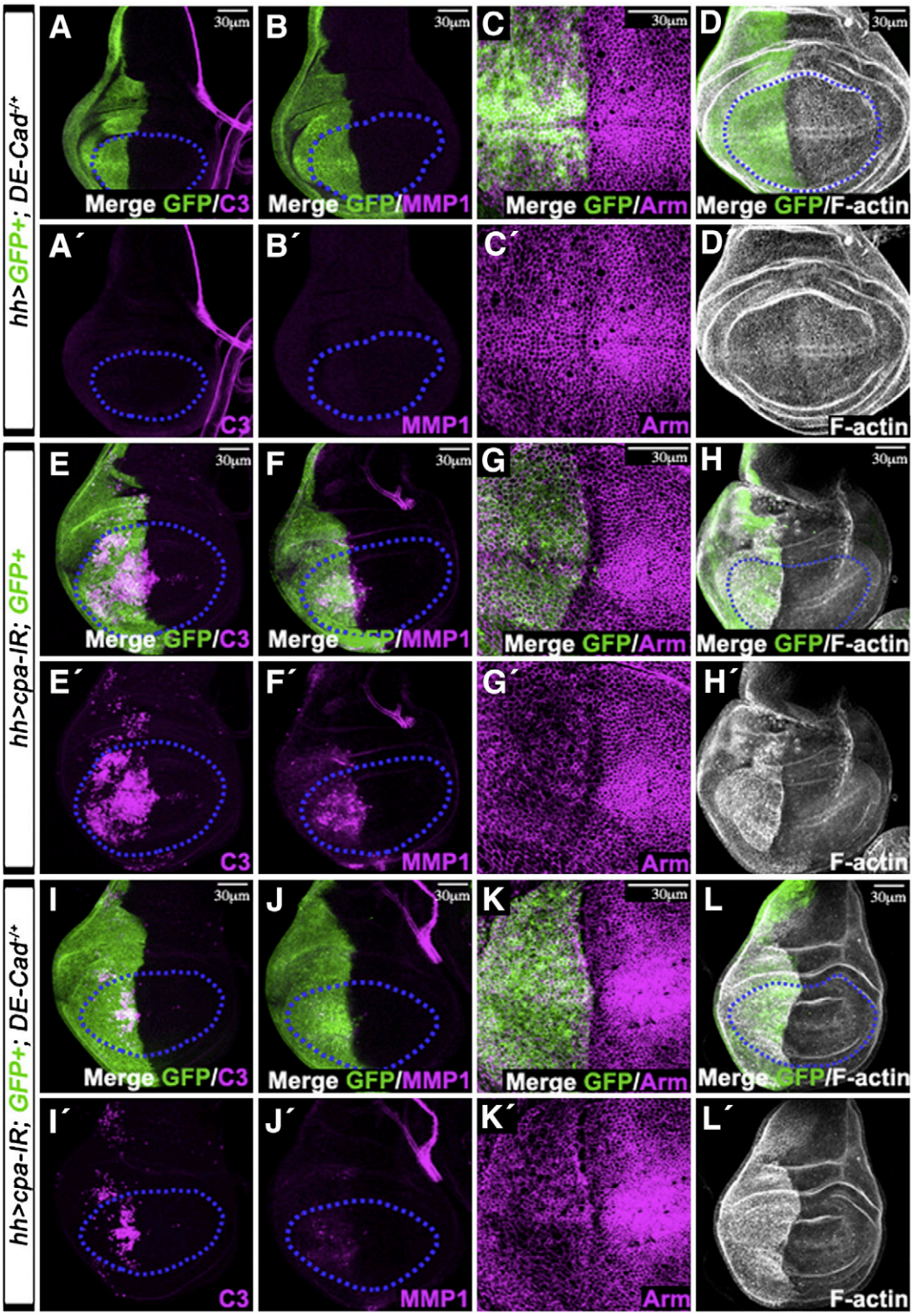

Fig. 5. Decreasing DE-Cad levels in Cpa-depleted cells prevents apoptosis and ectopic MMP1 expression but does not restore Arm at apical sites, nor suppresses F-actin accumulation. All panels show standard confocal sections of third instar wing imaginal discs with posterior side to the left and dorsal side up. (A–A′ to D–D′) discs heterozygote for *shg*^{k03401}, expressing UAS-*mCD8-GFP* (green in A, B, C and D) under *hh*-Gal4 control. (E–E′ to H–H′) wildtype discs expressing UAS-*cpa-IR*^{C10} and UAS-*mCD8-GFP* (green in E, F, G and H) under *hh*-Gal4 control. (I–I′ to L–L′) discs heterozygote for *shg*^{k03401}, expressing UAS-*cpa-IR*^{C10} and UAS-*mCD8-GFP* (green in I, J, K and L) under *hh*-Gal4 control. Discs are stained with (A–A′, E–E′ and I–I′) anti-C3 (magenta) or (B–B′, F–F′ and J–J′) anti-MMP1 (magenta) or (C–C′, G–G′ and K–K′) anti-Arm (magenta) or (D–D′, H–H′ and L–L′) Phalloidin to mark F-actin (white). The blue dashed lines outline the distal wing domains. Scale bars represent 30 μm.

compartments in each genetic background. *hh>cpa-IR* wing imaginal discs with two wildtype copies of *DE-cad* showed a reduction of 43% (n = 19) of the Sens signals in the posterior compartment. Removing one copy of *DE-cad* in this genetic background, partially restored the Sens signals up to 11% (32% reduction in the posterior compartment, $P<0.01$; n = 18). Taken together, these observations argue that DE-Cad triggers JNK-mediated apoptosis in CP-depleted cells by inhibiting Wg signalling.

Please cite this article as: Jezowska, B., et al., A dual function of *Drosophila* capping protein on DE-cadherin maintains epithelial integrity and prevents JNK-mediated apoptosis, Dev. Biol. (2011), doi:10.1016/j.ydbio.2011.09.016

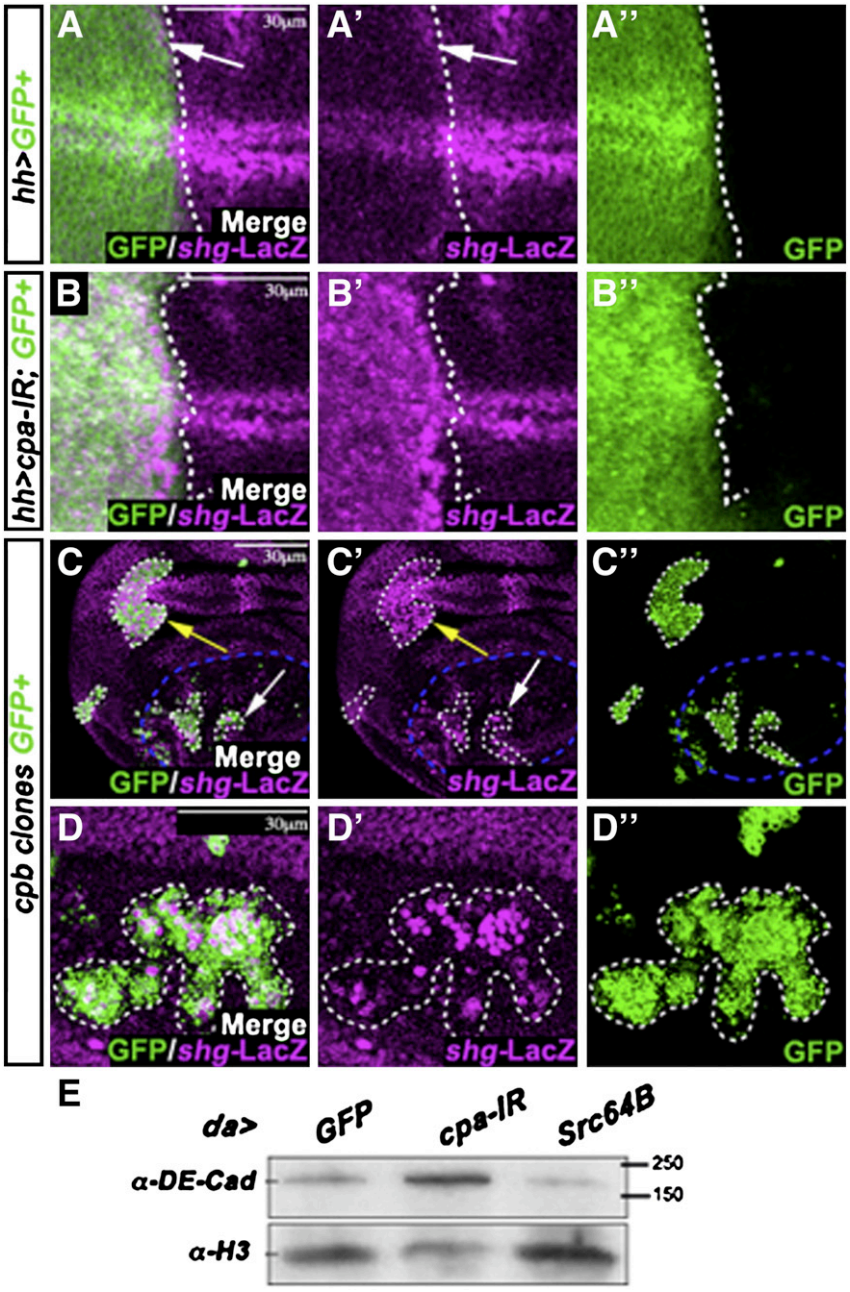

Fig. 6. Loss of CP upregulates *DE-cad* transcription and prevents DE-Cad protein accumulation. (A–A″ to D–D″) standard confocal sections of third instar wing imaginal discs with posterior side to the left and dorsal side up, stained with anti β-galactosidase to reveal *shg*-LacZ (magenta in A, A′, B, B′, C, C′, D and D′). (A–A″ and B–B″) discs carrying a *LacZ* insertion into the *shg* locus (shg^{k03401}) and expressing UAS-*mCD8-GFP* (green in A, A″, B and B″) and (B–B″) UAS-$cpa\text{-}IR^{C10}$ under *hh*-Gal4 control. The white dashed lines outline the A/P boundary. The white arrows in A and A′ indicate that increase *shg*-LacZ expression in posterior cells, apposed to the A/P boundary of control *hh>GFP* discs. Note that *shg*-LacZ expression is upregulated in cells with decreased CP levels. (C–C″ and D–D″) discs carrying a *LacZ* insertion into the *shg* locus (shg^{k03401}) and containing *hsFLP*-induced MARCM FRT40A, cpb^{M143} clones expressing *mCD8-GFP* (green in C, C″, D and D″). The blue dashed lines outline the distal wing domain. The white dashed lines outline *cpb* mutant clones. The yellow arrows in C and C′ indicate the increase *shg*-LacZ expression in *cpb* mutant clones that maintained a polarized epithelial architecture in the proximal wing domain. Scale bars represent 30 μm. (E) Western blot on protein extracts from first instar larvae expressing UAS-*mCD8-GFP* (lane 1) or UAS-$cpa\text{-}IR^{C10}$ (lane 2) or UAS-$Src64B^{UY1332}$ (lane 3) under *da*-Gal4 control, blotted with anti-DE-Cad (upper panel) and anti-H3 (lower panel). Note that in Cpa-depleted tissues, DE-Cad levels are increased.

The Ras oncogene induces massive proliferation of capping protein mutant cells

The results so far argue that in the distal wing disc epithelium, loss of CP affects cell polarity and triggers a DE-Cad-dependent signal, which induces JNK-mediated apoptosis. Activation of JNK signalling or inactivation of a number of genes affecting cell polarity has been shown to trigger tumour overgrowth when combined with activated Ras (Ras^{V12}) (Igaki et al., 2006; Leong et al., 2009; Pagliarini and Xu, 2003; Stockinger et al., 2001; Uhlirova and Bohmann, 2006). Therefore, expression of the Ras^{V12} oncogene might also be expected to switch the apoptotic response of CP mutant cells to a proliferative behaviour. In agreement with other reports (Karim and Rubin, 1998; Prober and Edgar, 2000, 2002), expressing the Ras^{V12} oncogene alone in clones positively labelled with GFP, led to epithelial outgrowths in the distal or proximal wing disc, characterized by the formation of cyst-like structures, described as "benign tumours", that expressed Arm at the apical cell surface (Figs. 8A, B–B′ and C–C′). While in the distal wing disc epithelium, *cpa* mutant clones extrude (Figs. 8D and E–E′) and die (Janody and Treisman, 2006), expressing Ras^{V12} in

Please cite this article as: Jezowska, B., et al., A dual function of *Drosophila* capping protein on DE-cadherin maintains epithelial integrity and prevents JNK-mediated apoptosis, Dev. Biol. (2011), doi:10.1016/j.ydbio.2011.09.016

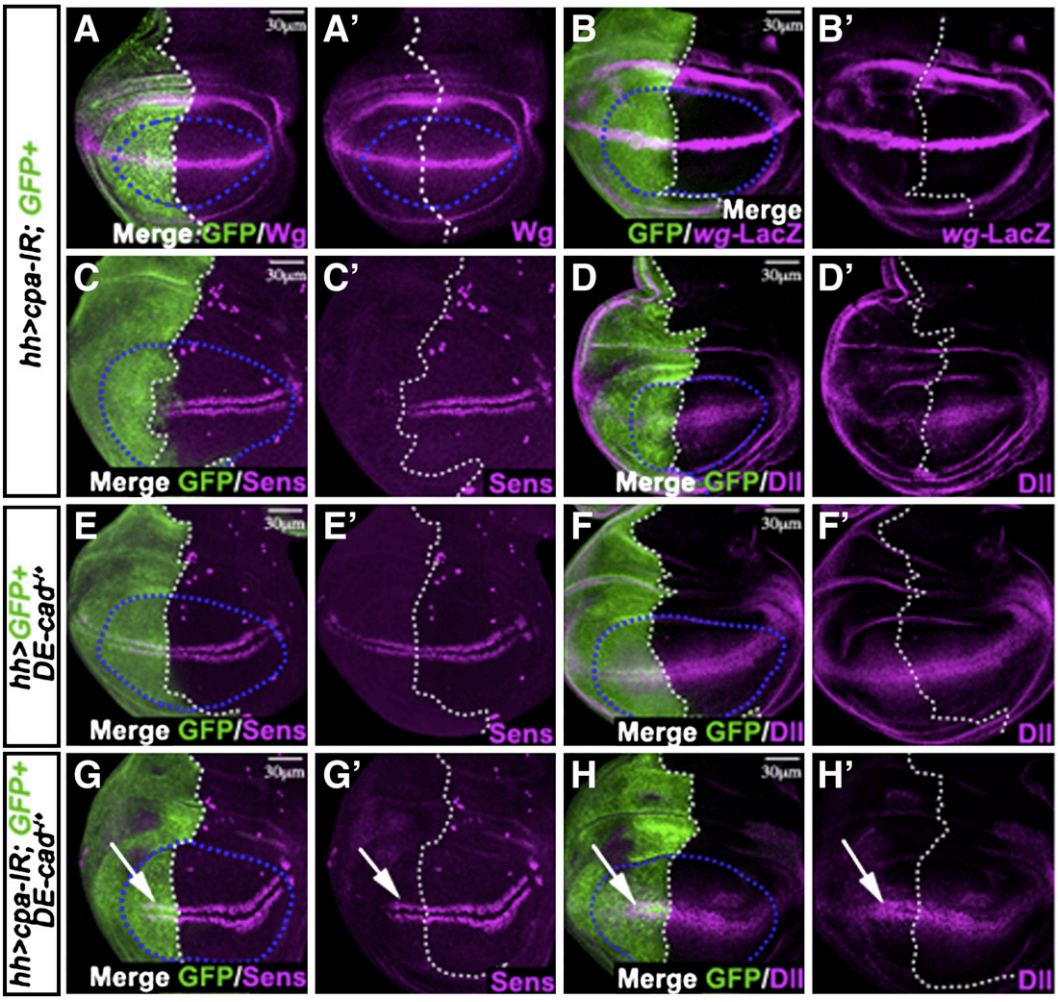

Fig. 7. Removing one copy of *DE-cad* in Cpa-depleted tissues restores Sens and Dll expression. All panels show standard confocal sections of third instar wing imaginal discs with posterior side to the left and dorsal side up. (A–A′ to D–D′) wildtype discs expressing UAS-*cpa-IR*^{C10} and UAS-*mCD8-GFP* (green in A, B, C and D) under *hh*-Gal4 control and (B–B′) carrying a *wg*-LacZ transgene. (E–E′ and F–F′) discs heterozygote for *shg*^{k03401}, expressing UAS-*mCD8-GFP* (green in E and F) under *hh*-Gal4 control. (G–G′ and H–H′) discs heterozygote for *shg*^{k03401}, expressing UAS-*cpa-IR*^{C10} and UAS-*mCD8-GFP* (green in G and H) under *hh*-Gal4 control. Discs are stained with (A–A′) anti-Wg (magenta) or (B–B′) anti-β-galactosidase to reveal *wg*-LacZ (magenta) or (C–C′, E–E′ and G–G′) anti-Sens (magenta) or (D–D′, F–F′ and H–H′) anti-Dll (magenta). The white dashed lines outline the A/P boundary. The blue dashed lines outline the distal wing domain. The white arrows in G, G′ and H, H′ indicate the recovery of Sens or Dll expression respectively in the posterior compartment expressing *cpa-IR* and heterozygote mutant for *DE-cad*. Scale bars represent 30 μm.

these cells triggered massive proliferation of cells localized basally (Fig. 8 compare G with D). Cross sections through the wing disc epithelium revealed that in the distal domain, *cpa* mutant cells expressing *Ras*^{V12} lost apically localized Arm and appeared multilayered (Figs. 8H–H′). In the proximal wing domain however, *cpa*$^{-/-}$; *Ras*^{V12}-expressing cells formed "benign tumours" that expressed Arm at the apical cell surface (arrows in Figs. 8I–I′), similar to wildtype cells expressing *Ras*^{V12} (arrows in Figs. 8B–B′ and C–C′). We conclude that in the distal wing epithelium, CP cooperates with Ras^{V12} to drive tissue overgrowth.

Blocking apoptosis of Cpa-depleted tissues triggers massive overgrowth

A number of studies have shown that Ras^{V12} subverts the pro-apoptotic response of JNK signalling into a potent inducer of tumour overgrowth (Igaki et al., 2006; Uhlirova and Bohmann, 2006). To investigate whether following CP loss JNK signalling can trigger cell proliferation when apoptosis is blocked, we expressed the baculovirus protein P35, which blocks the effector caspases. Expression of *P35* alone with *GFP* did not significantly induce ectopic pJNK (Figs. 9A–A′) but slightly upregulated expression of MMP1 (arrows in Figs. 9B–B′) and *msn*-LacZ (arrows in Figs. 9C–C′) in small patches. As expected, P35 expression prevented apoptosis of Cpa-depleted cells (compare Figs. S5E–E′ with C–C′) but did not suppress ectopic staining of pJNK (Figs. 9E–E″), MMP1 (Figs. 9F–F″) and *msn*-LacZ (Figs. 9G–G″). Therefore, in Cpa-depleted tissues kept alive with P35, JNK signalling is still active. Strikingly, expressing *cpa-IR* and *P35* under *hh* (Figs. 9E–E″ and F–F″) resulted in extensive overgrowth, characterized by the increased size of the posterior compartment, which became distorted and folded. Tissue overgrowth resulted from increased cell proliferation since the posterior compartment of *hh>cpa-IR; P35* wing imaginal discs contained more cells in mitosis when compared to the anterior compartment (Figs. 9H–H″). We also observed ectopic pH3 staining in wildtype anterior cells apposed to the *hh>cpa-IR; P35*-expressing domain (Figs. 9H–H′), indicating non-autonomous increase in cell proliferation. Transversal cross sections through *sd>cpa-IR; P35* wing disc showed that mitotic chromatin were not restricted to the apical cell surface but were found randomly distributed across the disc epithelium (arrows in Figs. 9I–I′). Moreover, these cells showed a rounded morphology (compare Figs. S5F with D and B), lost the appearance of a polarized columnar epithelium and appeared multilayered (compare Figs. 10E–E′ with B–B′).

Please cite this article as: Jezowska, B., et al., A dual function of *Drosophila* capping protein on DE-cadherin maintains epithelial integrity and prevents JNK-mediated apoptosis, Dev. Biol. (2011), doi:10.1016/j.ydbio.2011.09.016

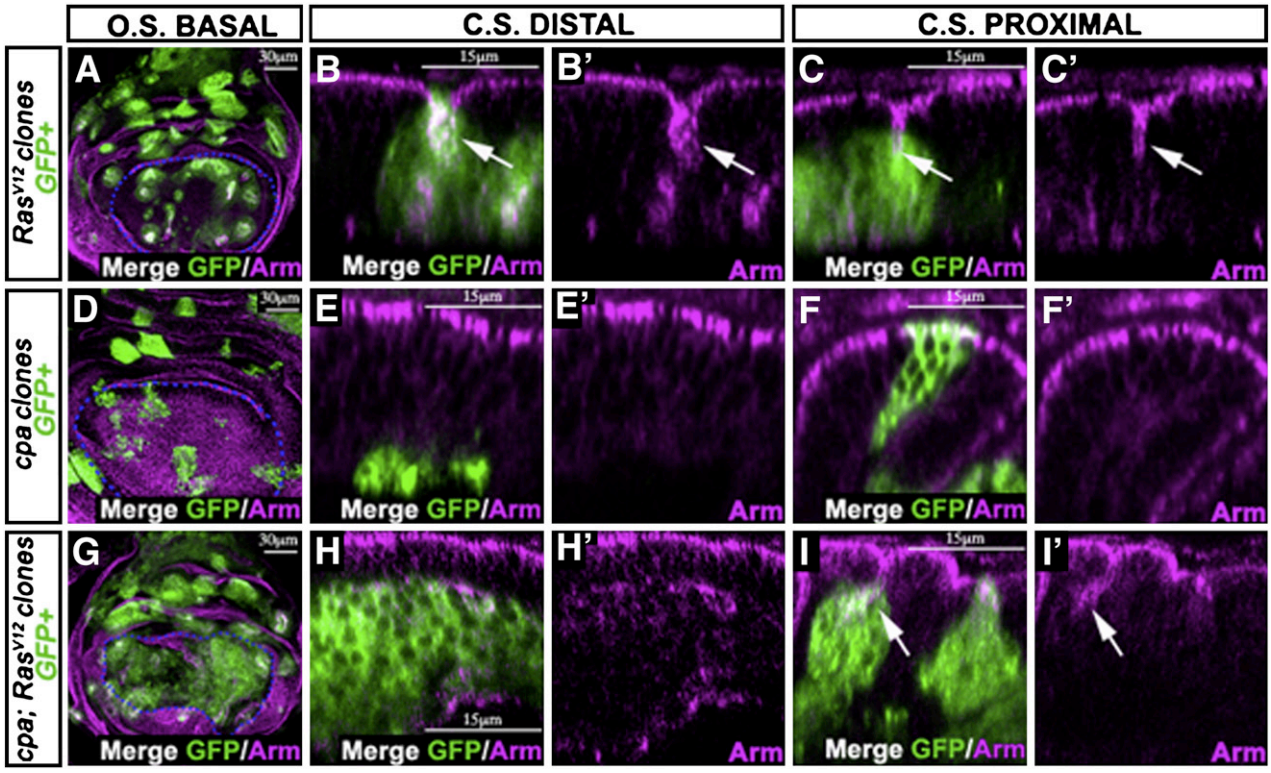

Fig. 8. Expressing Ras^{V12} induces massive proliferation of *cpa* mutant cells in the distal wing domain. All panels show third instar wing imaginal discs. (A, D and G) standard confocal sections with dorsal side up. (B–B′, C–C′, E–E′, F–F′, H–H′ and I–I′) optical cross sections through the (B–B′, E–E′ and H–H′) distal or (C–C′, F–F′ and I–I′) proximal disc epithelium with apical side up. (A to C–C′) clones expressing UAS-Ras^{V12} and UAS-*GFP* (green in A, B and C). (D to F–F′) cpa^{107E} mutant clones expressing UAS-*GFP* (green in D, E and F). (G to I–I′) cpa^{107E} mutant clones expressing UAS-Ras^{V12} and UAS-*GFP* (green in G, H and I). Discs are stained with anti-Arm (magenta). The blue dashed lines in A, D and G outline the distal wing disc domain. The white arrows in B, B′, C, C′, I and I′ indicate cyst-like structures. Scale bars represent 30 or 15 μm as indicated.

Some cells localized basally within the tissue, still expressed Arm in patches (white arrow in Fig. 10E′), while others lost Arm and detached from their neighbours, forming discontinuities within the tissue (yellow arrow in Fig. 10E). In control, expressing *P35* under *sd*-Gal4 control had little effect on epithelial architecture (Figs. 10A–A′, B–B′ and Fig. S5B). Finally, in contrast to *sd>P35* control tissues (Figs. 10C–C′), *cpa-IR; P35*-expressing cells also upregulated N-Cadherin (N-Cad) (Figs. 10F–F′). We conclude that Cpa-depleted cells kept alive with P35 fail to stably retain associations with their neighbours and overproliferate.

JNK and Yki trigger overgrowth of "undead" capping protein-depleted tissues

We then tested whether overgrowth of "undead" Cpa-depleted tissues involved JNK signalling. Expression of bsk^{DN} did not affect the outcome of P35-expressing tissues (Figs. 10G–G′) but suppressed tissue overgrowth and ectopic N-Cad expression when tissues where also knocked down for Cpa (Figs. 10H–H′). Therefore, following loss of CP, activation of JNK signalling triggers massive cell death but acts as potent inducer of proliferation when Cpa-depleted cells are kept alive with P35. Cell death in response to stress and damage can also induce JNK-dependent compensatory proliferation (Fan and Bergmann, 2008). Subjecting *sd>GFP* larvae to non-lethal heat shock induced high apoptotic levels in imaginal discs (Figs. S5G–G″) or morphological aberrations when cells were kept alive with expression of P35 (Figs. S5H–H′). However unlike "undead" Cpa-depleted tissues, heat shocked *sd>GFP; P35* wing discs did not display extensive overgrowth of the distal domain and maintained a stratified epithelial organization (compare Fig. S5I with F). Thus, overgrowth of *cpa-IR, P35*-expressing cells is unlikely to result only from stress-induced compensatory proliferation. Instead, our observations suggest that in cells lacking CP, the defect in cell–cell adhesion enhances JNK-mediated proliferation.

Loss of CP or induction of JNK signalling promotes activation of the Yki oncogene in the wing imaginal disc (Fernandez et al., 2011; Sansores-Garcia et al., 2011; Sun and Irvine, 2011). We therefore tested the role of Yki, downstream of JNK in proliferation of "undead" Cpa-depleted cells. Reduction of Yki protein by RNAi prevented growth of P35-expressing tissues (Figs. 10I–I′) and rescued the overgrowth response due to expression of P35 in Cpa-depleted cells (Fig. 10 compare J with D–D′). Moreover, while decreasing Yki levels in "undead" Cpa-depleted cells fully suppressed N-Cad upregulation (Fig. 10 compare J′ with F–F′), it did not prevent F-actin accumulation, nor fully suppress ectopic expression of MMP1 (Figs. S6B–B′). These observations indicate that Yki is required for overgrowth of CP-depleted tissues kept alive with P35 and suggest that the pro-growth function of JNK signalling requires Yki activity.

Discussion

Regulation of JNK-mediated apoptosis or proliferation by capping protein

In this study, we demonstrate that in the distal wing disc epithelium, JNK signalling triggers apoptosis of cells with reduced CP expression (Figs. 2, 3, 4 and Model in Fig. 11A) but induces massive proliferation when apoptosis is blocked with P35 (Figs. 9, 10 and Model in Fig. 11B). Yki activity is also required to allow overgrowth of "undead" Cpa-depleted tissues (Fig. 10). Induction of apoptosis has been shown to activate Yki through the JNK pathway and triggers compensatory cell proliferation (Sun and Irvine, 2011). Thus, in CP-depleted cells kept alive with P35, Yki may act downstream of JNK

Please cite this article as: Jezowska, B., et al., A dual function of *Drosophila* capping protein on DE-cadherin maintains epithelial integrity and prevents JNK-mediated apoptosis, Dev. Biol. (2011), doi:10.1016/j.ydbio.2011.09.016

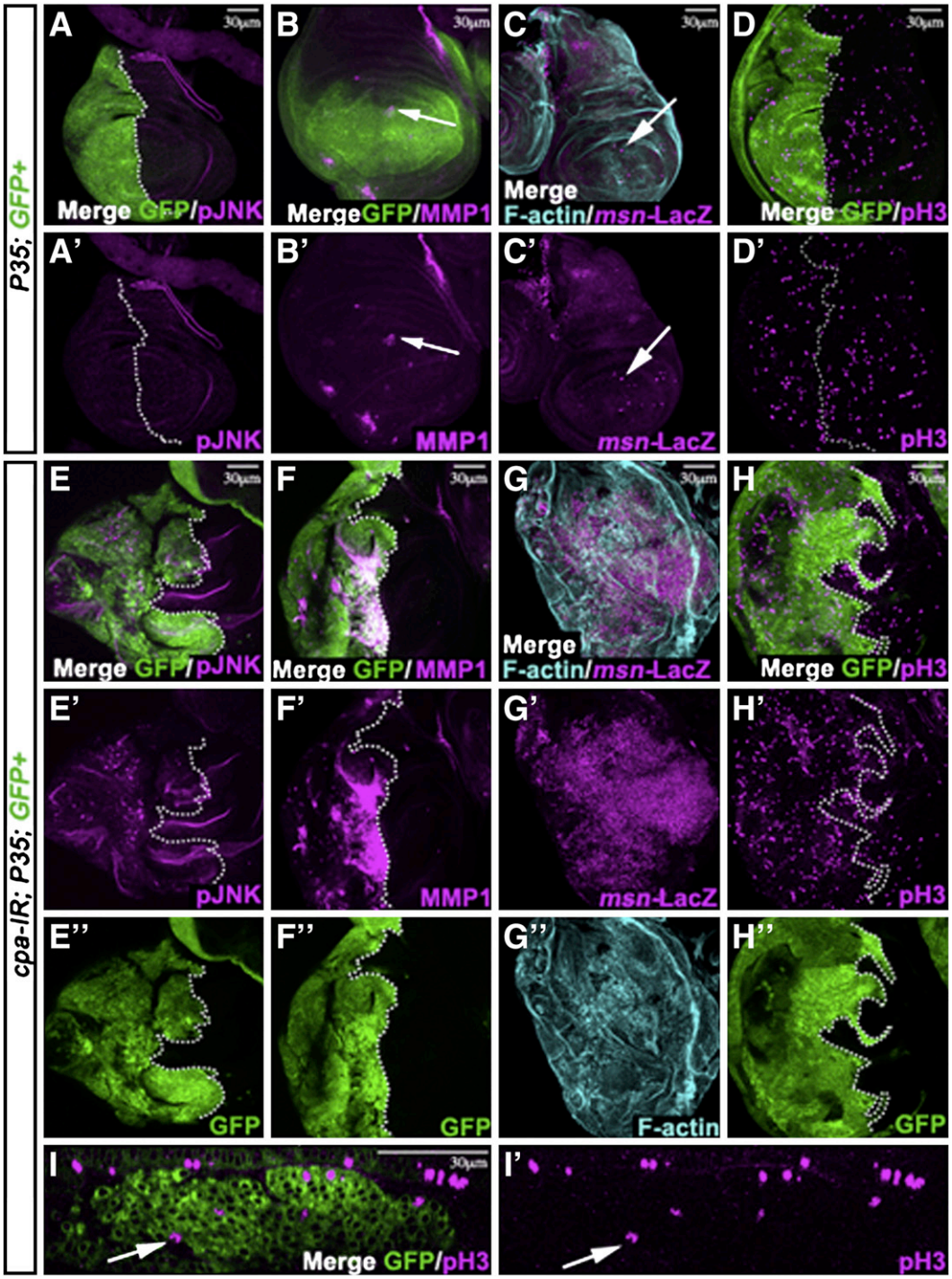

Fig. 9. Expressing *P35* in Cpa-depleted cells triggers tissue overgrowth but does not suppress activation of JNK signalling. All panels show third instar wing imaginal discs. (A–A′ to H–H″) standard confocal sections with posterior side to the left and dorsal side up. (I–I′) optical cross sections through the disc epithelium with apical side up. (A–A′ to D–D′) discs expressing UAS-*mCD8-GFP* (green in A, B and D) and UAS-*P35* under (A–A′ and D–D′) *hh*-Gal4 or (B–B′ and C–C′) *sd*-Gal4 control, and (C–C′) carrying a *LacZ* insertion into the *msn* (msn^{06946}) locus. The white arrows in B–B′ and in C–C′ indicate ectopic expression of *msn*-LacZ and MMP1 respectively. (E–E″ to I–I′) discs expressing UAS-*mCD8-GFP* (green in E, E″, F, F″, H, H″ and I), UAS-*P35* and UAS-*cpa-IR*^{C10} under (E–E″, F–F″ and H–H″) *hh*-Gal4 or (G–G″ and I–I′) *sd*-Gal4 control, and (G–G″) carrying a *LacZ* insertion into the *msn* (msn^{06946}) locus. Discs are stained with (A–A′ and E–E″) anti-pJNK (magenta in A, A′, E and E′) or (B–B′ and F–F″) anti-MMP1 (magenta in B, B′, F and F′) or (C–C′ and G–G″) anti β-galactosidase to reveal *msn*-LacZ (magenta in C, C′, G and G′) and Phalloidin (cyan in C, G and G″) or (D–D′, H–H″ and I–I′) anti-pH3 (magenta in D, D′, H, H′, I and I′). The white arrows in I–I′ indicate mitotic chromatin randomly distributed across the disc epithelium. The white dashed lines in A–A′, D–D′, E–E″, F–F″ and H–H″ outline the border between the posterior cells, expressing *GFP* and *cpa-IR*, and the anterior wildtype cells. Scale bars represent 30 μm.

signalling. Consistent with this, targeting Yki degradation in these tissues fully suppresses ectopic N-Cad expression (Fig. 10) but not MMP1 upregulation (Fig. S6). Because CP also prevents Yki activity in the whole wing disc epithelium, independently of its effect on JNK signalling, (Fernandez et al., 2011; Sansores-Garcia et al., 2011), in the distal wing domain, excess Yki activity of "undead" CP-depleted tissues may result from a dual effect, which involves a JNK-dependent and independent mechanisms.

JNK signalling has been reported to propagate from cell to cell in the wing disc, where it could trigger apoptosis or Yki-dependent compensatory proliferation (Sun and Irvine, 2011; Wu et al., 2010). We did not observe non-autonomous apoptosis or activation

Please cite this article as: Jezowska, B., et al., A dual function of *Drosophila* capping protein on DE-cadherin maintains epithelial integrity and prevents JNK-mediated apoptosis, Dev. Biol. (2011), doi:10.1016/j.ydbio.2011.09.016

of JNK signalling when we induced patches of CP mutant cells or expressed dsRNA for CP with or without P35 (Figs. 2, 3, 9 and Janody and Treisman, 2006). Therefore, the propagation of JNK activation might be impaired in tissues knocked down for CP. However, we observed increase proliferation of wildtype cells apposed to "undead" Cpa-depleted tissues (Fig. 9). This suggests that JNK propagation is not required to trigger compensatory cell proliferation.

Several observations argue that in cells lacking CP, a DE-Cad-dependent signal promotes JNK-mediated apoptosis by inhibiting Wg signalling. First, knocking down Cpa affects Wg signalling (Fig. 7), which has been shown to prevent JNK-dependent cell death in this region (Adachi-Yamada et al., 1999). Second, removing one copy of *DE-cad* in Cpa-depleted cells partially suppresses apoptosis and ectopic MMP1 expression (Fig. 5) and restores Wg target genes expression (Fig. 7). Third, loss of CP is associated with upregulation of the *DE-cad* gene and increased levels of the DE-Cad protein (Fig. 6). One way by which DE-Cad may block Wg signalling is by tethering Arm. In agreement with this possibility, in the distal wing disc epithelium, overexpression of *DE-cad* compromises Wg signalling, while co-expression of Arm rescues the *DE-cad* overexpression phenotype (Sanson et al., 1996; Widmann and Dahmann, 2009). Moreover, in mouse, overexpression of *E-Cad* induces apoptosis (Hermiston et al., 1996) and sequesters the transcriptionally competent pool of β-cat, effectively shutting off expression of Lef/TCF/β-cat-responsive genes (Gottardi et al., 2001; Orsulic et al., 1999; Stockinger et al., 2001). Interestingly, in Cpa-depleted tissues, the faster mobility form of Arm is enriched (Fig. 1). Because this form was proposed to correspond to the cytoplasmic pool of Arm (Peifer et al., 1994), following CP loss, increase DE-Cad levels might tether and stabilize Arm in the cytoplasm, preventing it to transduce Wg signalling. How a defect in Wg signalling triggers JNK-mediated cell death is not known. Consistent with previous reports (Kuranaga et al., 2002; Ryoo et al., 2004), in cells lacking CP, JNK activation may occur in response to loss of DIAP1 since overexpressing *DIAP1* strongly reduces ectopic MMP1 expression (Figs. 2 and S3). However, we cannot exclude that JNK signalling reduces DIAP1 levels since JNK signalling can also function upstream of DIAP1 (Igaki, 2009).

Capping protein has a dual function on DE-cadherin

In the distal wing domain, cells lacking CP mislocalize DE-Cad and Arm at AJs, upregulate expression of *DE-cad* and extrude from the epithelium (Figs. 1, 6 and Janody and Treisman, 2006). *DE-cad* appears to be a direct transcriptional target of the Hpo signalling pathway (Genevet et al., 2009). CP inhibits Yki activity (Fernandez et al., 2011; Sansores-Garcia et al., 2011) and prevents *shg*-LacZ upregulation, even in mutant

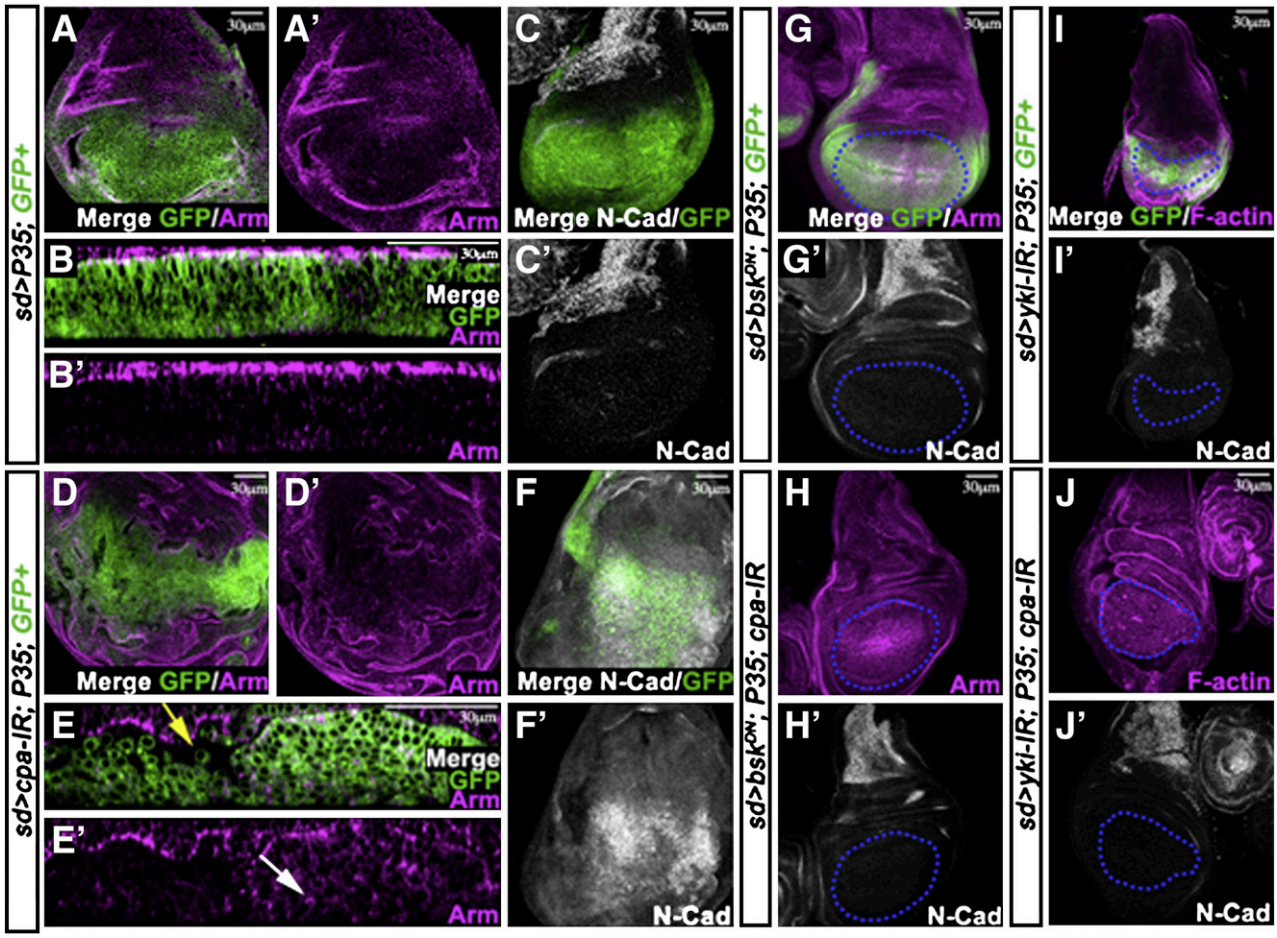

Fig. 10. Expressing *bsk*^{DN} or *yki-IR* suppresses tissue overgrowth and ectopic N-Cad expression of "undead" Cpa-depleted tissues. All panels show third instar wing imaginal discs. (A–A′, C–C′, D–D′, F–F′ and G–G′ to J–J′) standard confocal sections with dorsal side up. (B–B′ and E–E′) optical cross sections through the distal disc epithelium with apical side up. (A–A′ to C–C′) *sd*-Gal4 driving UAS-*mCD8-GFP* (green in A, B and C) and UAS-*P35*. (D–D′ to F–F′) *sd*-Gal4 driving UAS-*mCD8-GFP* (green in D, E and F), UAS-*P35* and UAS-*cpa-IR*^{C10}. Discs are stained with (A–A′ B–B′, D–D′) anti-Arm (magenta) or (C–C′ and F–F′) anti-N-Cad (white). The yellow arrow in E indicates a Cpa-depleted cell expressing P35 and GFP, which lost Arm and detached from other cells. The white arrow in E′ indicates a Cpa-depleted cell expressing P35 and GFP, which localized basally within the tissue and expressed Arm in patches. (G–G′) *sd*-Gal4 driving UAS-*mCD8-GFP* (green in G), UAS-*bsk*^{DN} and UAS-*P35*. (H–H′) *sd*-Gal4 driving UAS-*bsk*^{DN}, UAS-*P35* and UAS-*cpa-IR*^{C10}. Discs are stained with anti-Arm (magenta in G and H) and anti-N-Cad (white in G′ and H′). (I–I′) *sd*-Gal4 driving UAS-*mCD8-GFP* (green in I), UAS-*yki-IR*$^{4005R-2}$ and UAS-*P35*. (J–J′) *sd*-Gal4 driving UAS-*yki-IR*$^{4005R-2}$, UAS-*P35* and UAS-*cpa-IR*^{C10}. Discs are stained with Phalloidin to mark F-actin (magenta in I and J) and anti-N-Cad (white in I′ and J′). The blue dashed lines in G–G′ to J–J′ outline the distal wing disc domain. Scale bars represent 30 μm.

Please cite this article as: Jezowska, B., et al., A dual function of *Drosophila* capping protein on DE-cadherin maintains epithelial integrity and prevents JNK-mediated apoptosis, Dev. Biol. (2011), doi:10.1016/j.ydbio.2011.09.016

clones that maintain a polarized epithelial architecture in the proximal wing domain (Fig. 6). Thus, increased *DE-cad* expression likely results from inhibition of Hpo pathway activity. However, while mutant clones for Hpo pathway components accumulate DE-Cad, mutant cells do not extrude from the wing disc epithelium (Genevet et al., 2009; Maitra et al., 2006). Therefore, the polarity defect of cells lacking CP is unlikely to result from increased DE-Cad levels. Different observations also argue that altered cell–cell adhesion does not result from a defect in Wg signalling or from ectopic activation of JNK signalling, as previously reported (Igaki et al., 2006; Jaiswal et al., 2006; Uhlirova and Bohmann, 2006; Widmann and Dahmann, 2009). First, reducing *DE-cad* levels do not restore Arm localization at AJs (Fig. 5). Second, in Cpa-depleted tissues in which JNK signalling is blocked, dividing nuclei surrounded by dense F-actin patches are recovered on the basal surface of the distal wing disc epithelium (Fig. 4). Third, unlike cells lacking CP, tissues expressing P35 and defective for Wg signalling or overexpressing *DE-cad* or in which high apoptotic levels were induced maintain a polarized epithelial architecture (Figs. 10, S5, and Widmann and Dahmann, 2009). Therefore, following loss of CP, the mislocalization of DE-Cad and Arm and the loss of cell–cell contacts are likely upstream or parallel events to *DE-cad* upregulation and JNK-mediated cell death. Because disruption of apical–basal polarity can trigger JNK activation (Igaki et al., 2006; Uhlirova and Bohmann, 2006), we favour a model by which CP prevents JNK-mediated cell death though a dual function on DE-Cad: it promotes DE-Cad-mediated cell adhesion and restricts *DE-cad* expression (Fig. 11A).

While the effect of CP loss on *DE-cad* transcription is not context dependent, the polarity defect is mainly observed in the distal wing domain. Different regions of the wing disc may have specific requirements in terms of AJs stability and remodelling. Because the distal wing disc is under higher mechanical stress (Aegerter-Wilmsen et al., 2007, 2010; Nienhaus et al., 2009), this epithelium may require higher dynamics of DE-Cad remobilization. CP might be critical to control this kinetic, making distal wing cells lacking CP more prone to lose cell–cell adhesion and extrude from the epithelium.

Interestingly, the proto-oncogene of the Src family kinases Src42A antagonizes DE-Cad-mediated cell adhesion and stimulates the transcription of *DE-cad* (Shindo et al., 2008). Moreover, in the distal wing disc epithelium, the major inhibitor of Src family kinases C-terminal Src kinase (Csk), maintains AJs stability, prevents JNK-mediated apoptosis, whereas halving the genetic dose of *DE-cad* suppresses the apoptotic phenotype of dCsk-depleted cells (Vidal et al., 2006). CP and mammalian c-Src both regulate F-actin (Cooper and Sept, 2008; Frame, 2004). Conversely, the control of F-actin impacts on the kinase activity of c-Src (Desprat et al., 2008; Giannone and Sheetz, 2006; Kim et al., 2009). Thus, whether the main role of CP is to regulate Src activity in the distal wing disc is an exciting possibility to be tested in the future.

Actin-capping protein and tumour development

We and others have previously shown that the CP heterodimer acts as tumour suppressor through its control of Hpo pathway activity (Fernandez et al., 2011; Sansores-Garcia et al., 2011). We show now that in specific epithelia, loss of CP also affects cell–cell adhesion (Fig. 1), which is a fundamental step to an epithelial-to-mesenchymal transition (EMT) (Dow and Humbert, 2007), triggers MMP1 expression (Fig. 3), which degrades the basal extracellular matrix (Minn et al., 2005), induces cell invasion (Figs. 1 and S1) and promotes massive proliferation of cells that fail to stably retain associations with their neighbours when cell death is blocked with P35 (Figs. 9 and 10). Moreover "undead" CP-depleted cells show ectopic N-Cad expression, whose *de novo* expression promotes the transition from a benign to a malignant tumour phenotype (Cavallaro and Christofori, 2004). Finally, like other tumour suppressor (Brumby and Richardson, 2003; Igaki et al., 2006; Pagliarini and Xu, 2003; Vidal et al., 2007), loss of *CP* cooperates with Ras^{V12} in tissue overgrowth (Fig. 8). These findings argue that in some epithelia in which CP activity is affected, the appearance of a second mutation that prevents apoptotic cell death may trigger the development of aggressive tumours in humans. However, in contrast to tumour progression, which correlates with loss of overall E-Cad expression and stimulation of canonical Wnt signalling (Jeanes et al., 2008), we observed increase DE-Cad levels (Fig. 6) and inhibition of Wg signalling (Fig. 7) in tissues knocked down for CP. Interestingly, in flies, *shg*-LacZ expression is also enhanced in response to ectopic expression of the two oncogenes Src42A and Yki (Genevet et al., 2009; Shindo et al., 2008). This suggests the interesting hypothesis that transcriptional stimulation of *DE-cad* is an early mechanism of tumour suppression, which would promote the elimination of deleterious cells, possibly through inhibition of Wg signalling, rather than allowing them to proliferate and form tumours. Malignant cells that become resistant to cell death may compete successfully by losing the overall E-Cad expression

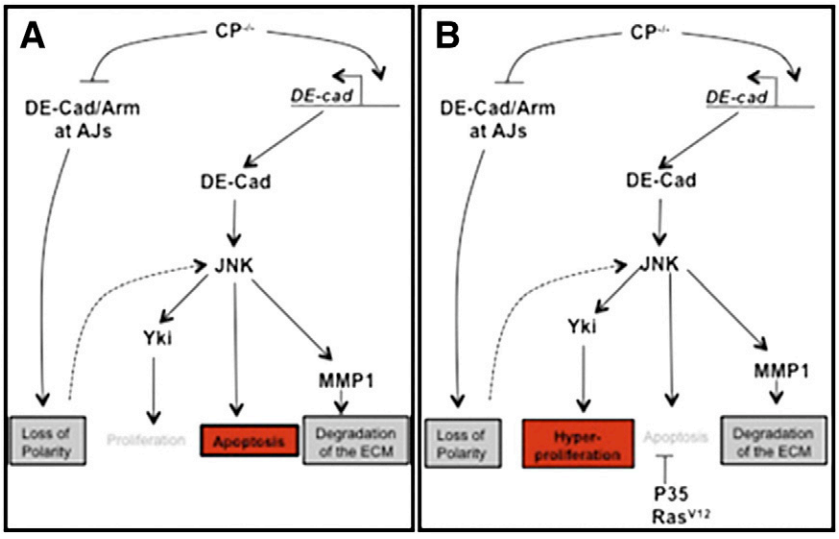

Fig. 11. Model through which loss of CP triggers apoptosis or massive overgrowth in the distal wing domain. (A) Loss of *CP* enhances transcription of the *DE-cad* gene and mislocalizes DE-Cad and Arm at AJs, which triggers loss of epithelial cell polarity. Both inputs might contribute to promote JNK-mediated apoptosis and degradation of the extracellular matrix (ECM) through ectopic expression of MMP1. (B) Expressing P35 or Ras^{V12} in cells lacking CP blocks apoptosis and unveils a role of JNK in promoting massive proliferation, possibly though Yki activation.

Please cite this article as: Jezowska, B., et al., A dual function of *Drosophila* capping protein on DE-cadherin maintains epithelial integrity and prevents JNK-mediated apoptosis, Dev. Biol. (2011), doi:10.1016/j.ydbio.2011.09.016

and upregulating mesenchymal cadherins such as N-Cad to reinforce their fitness.

Materials and methods

Fly strains and genetics

To generate wildtype or *cpa* mutant clones marked by the absence of GFP in the wing disc, in a manner that permits the recovery of cells within the distal wing epithelia at the end of third instar, *y, w*; FRT42D, *cpa*/CyO P(y^+) or y, w; FRT42 males were crossed to *y, w*, FRT42D, *ubi*-GFP; *T155*-Gal4, UAS-*flp*/ST females. Because *T155*-Gal4 directs expression of the UAS-*flp* at all larval stages, this permitted to catalyse continuous mitotic recombination between the chromatid carrying the FRT wildtype or *cpa* mutant allele and its GFP–marked wildtype homolog until the end of third instar. To generate *cpb* mutant clones positively labelled with GFP, *y, w*; FRT40A, *cpb*/CyO P (y^+) males were crossed to *y, w*, *hs*FLP122, UAS-*GFP*; FRT40A, *tub*-Gal80; *tub*-Gal4/TM6β females. The offspring were heat-shocked for 1 h at 37 °C at both 24 and 48 h after a 24 hour egg collection, corresponding to the first and second larval instar. To generate clones positively labelled with GFP, mutant for *cpa* or expressing Ras^{V12} or mutant for *cpa* and expressing Ras^{V12}, *y, w*; FRT42D, *cpa*/CyO P(y^+) or FRT42D, *cpa*/CyO P(y^+); UAS-Ras^{V12}/TM6β or FRT42D; UAS-Ras^{V12}/TM6β males were crossed to *y, w*, *hs*FLP122, UAS-*GFP*; FRT42D, *tub*-GAL80; *tub*-GAL4/TM6B. The offspring were heat shocked for 15 min 48 h after a 24 hours egg collection, corresponding to the second larval instar. All crosses were maintained at 22 °C. Fly stocks used were cpa^{107E}; cpb^{M143}; UAS-*HA-cpa* (Janody and Treisman, 2006); UAS-*cpa*-IR^{C10} (Fernandez et al., 2011); UAS-*cpa*-IR^{100773}; UAS-*cpb*-IR^{45668} (Vienna *Drosophila* Research Center, VDRC); UAS-*cpa*-IR^{7009}; UAS-*yki*-$IR^{4005R-2}$ (National Institute of Genetics, NIG); $Src64B^{UY1332}$ (Nicolai et al., 2003); UAS-Ras^{V12} (Karim and Rubin, 1998); UAS-*DIAP1* (Ryoo et al., 2002); UAS-*P35* (Hay et al., 1994); UAS-bsk^{DN} (Adachi-Yamada et al., 1999); *puc-lacZ* (puc^{E69}) (Martin-Blanco et al., 1998); *msn*-LacZ (msn^{06946}) (Spradling et al., 1999); shg^{k03401} (Uemura et al., 1996); cad^2 (Tepass et al., 1996); *sd*-Gal4 (Klein and Arias, 1998); *hh*-Gal4, a gift from T. Tabata; *da*-Gal4 (Wodarz et al., 1995); *en*-Gal4 (Brodsky et al., 2000; Ollmann et al., 2000); *ptc*-Gal4 (Tang and Sun, 2002).

Immunohistochemistry

We performed immunocytochemistry on the wing imaginal disc of third instar larvae using the procedure described in Lee and Treisman (2001). Between 15 and 30 discs were analysed for each genetic combination. Antibodies used were mouse anti-Arm (N2 7A1, 1:10; DSHB), rat anti-DE-Cad (CAD2; 1:50, DSHB), rabbit anti-Hth (1:500; Kurant et al., 1998), guinea pig anti-Hth (1:3000; Casares and Mann, 1998), rabbit anti-activated Caspase 3 (1:500; BD Bioscience), mouse anti-MMP1 (cocktail 1:1 of 5H7B11 and 3B8D12; 1:50, DSHB), rat anti-N-Cad (DN-Ex#8; 1:10 DSHB), mouse anti-DIAP1 (1:200 from B. Hay), rabbit anti-pJNK (1:50 Promega); mouse anti-Wg (4D4; 1:10, DSHB); guinea pig anti-Sens (1:1000; Nolo et al., 2000); rabbit anti-Dll (1:200; Panganiban et al., 1995); mouse anti-β-galactosidase (1:200; Promega), rabbit anti-phosphorylated Histone 3 (Cell Signalling 1:200). TOTO 3 (Alfagene) was used at 1:1000. Rhodamine-conjugated Phalloidin (Sigma) was used at a concentration of 0.3 μM. Secondary antibodies were from Jackson Immunoresearch, used at 1:200 (donkey anti-rabbit TRITC #711-025-152; donkey anti-rabbit Cy™5 #711-175-152; donkey anti-mouse Cy™5 #715-175-150; donkey anti-mouse TRITC #715-025-151; donkey anti-rat TRITC #712-025-153; donkey anti-guinea pig TRITC #706-025-148). Fluorescence images were obtained on a Leica SP5 TCS NT or a LSM 510 Zeiss confocal microscope using either a 20× dry or 40× oil objectives. The NIH Image J program was used to perform measurements. To quantify the intensity of Caspase 3 signals, the posterior and anterior compartment of *hh*>$shg^{+/+}$; *cpa*-IR^{C10} and *hh*>$shg^{k03401/+}$; *cpa*-IR^{C10} wing discs were outlined separately for each disc and the intensity levels were calculated as the sum of the grey values of all the pixels in the selection divided by the number of pixels for each compartment. To quantify the intensity of Sens signals, a region of interest (ROI) of 90 per 90 pixels (around 35 cells) was selected. The sum of the grey values was measured for each ROI, applied on the D/V compartment boundary that comprises the Sens staining, on each side of the posterior and anterior compartments on standard confocal sections merging the entire Sens signals. The ratio of signal between the posterior and anterior compartments was calculated for each disc. Statistical significance was calculated using a two-tailed *t*-test.

Western blotting

For each genotype, either wildtype (w^{1118}) or expressing UAS-*GFP* or UAS-*cpa*-IR^{C10} or UAS-$Src64B^{UY1332}$ under the control of *daughterless*-GAL4 (*da*-Gal4), proteins were extracted from either 5 embryos (20 to 24 h old) or 10 first instar larvae. Larvae were homogenized in 5 μl of lysis buffer (50 mM Tris pH 7.4, 150 mM NaCl, 1 mM EDTA pH 7.4, 1% NP-40) in the presence of protease inhibitors (Roche #04693159001) and phosphatase inhibitors (Sigma #S 6508 and S 7920). Samples were frozen in liquid nitrogen, boiled for 5 min in 5 μl sample buffer 2×, spun at 13,000 *g* for 1 min, loaded on a 10% SDS-PAGE gel and transferred to a PVDF membrane (Amersham Hybond™-P, GE Healthcare). Proteins were visualized by immunoblotting using rabbit anti-H3 (1:1000; Cell Signalling) and mouse anti-Arm (1:100; DSHB) or Rat anti-DE-Cad (1:200; DSHB). To quantify the relative amounts of Arm Protein in each genetic background, Western blots were scanned and analysed using the Image J software (NIH; http://rsb.info.nih.gov/ij/). Following a background correction step, the intensity levels of the Arm or DE-Cad signals were calculated as the sum of the grey values of all the pixels in the selection. Values were then normalized with those of the anti-H3 signals.

Supplementary materials related to this article can be found online at doi:10.1016/j.ydbio.2011.09.016.

Acknowledgments

We thank T. Xu, B. Hay, R. Mann, A. Laughon, G. Morata, the Bloomington *Drosophila* Stock Center, the National Institute of Genetics and the Developmental Studies Hybridoma Bank for fly stocks and reagents. The manuscript was improved by the critical comments of Pedro Gaspar, Vitor Barbosa, Rui Martinho, Monica Bettencourt-Dias, Elodie Mohr and Christen Mirth. This work was supported by grants from Fundação para a Ciência e Tecnologia (Grants PTDC/SAU-OBD/73191/2006 and PTDC/BIA-BCM/71674/2006). B.G.F. and B.J. were the recipients of fellowships from Fundação para a Ciência e Tecnologia (SFRH/BPD/35915/2007 and SFRH/BD/33215/2007 respectively).

References

Adachi-Yamada, T., Fujimura-Kamada, K., Nishida, Y., Matsumoto, K., 1999. Distortion of proximodistal information causes JNK-dependent apoptosis in *Drosophila* wing. Nature 400, 166–169.

Aegerter-Wilmsen, T., Aegerter, C.M., Hafen, E., Basler, K., 2007. Model for the regulation of size in the wing imaginal disc of *Drosophila*. Mech. Dev. 124, 318–326.

Aegerter-Wilmsen, T., Smith, A.C., Christen, A.J., Aegerter, C.M., Hafen, E., Basler, K., 2010. Exploring the effects of mechanical feedback on epithelial topology. Development 137, 499–506.

Assemat, E., Bazellieres, E., Pallesi-Pocachard, E., Le Bivic, A., Massey-Harroche, D., 2008. Polarity complex proteins. Biochim. Biophys. Acta 1778, 614–630.

Baker, N.E., 1988. Transcription of the segment-polarity gene wingless in the imaginal discs of *Drosophila*, and the phenotype of a pupal-lethal wg mutation. Development 102, 489–497.

Brodsky, M.H., Nordstrom, W., Tsang, G., Kwan, E., Rubin, G.M., Abrams, J.M., 2000. *Drosophila* p53 binds a damage response element at the reaper locus. Cell 101, 103–113.

Please cite this article as: Jezowska, B., et al., A dual function of *Drosophila* capping protein on DE-cadherin maintains epithelial integrity and prevents JNK-mediated apoptosis, Dev. Biol. (2011), doi:10.1016/j.ydbio.2011.09.016

Brumby, A.M., Richardson, H.E., 2003. Scribble mutants cooperate with oncogenic Ras or Notch to cause neoplastic overgrowth in *Drosophila*. EMBO J. 22, 5769–5779.

Casares, F., Mann, R.S., 1998. Control of antennal versus leg development in *Drosophila*. Nature 392, 723–726.

Cavallaro, U., Christofori, G., 2004. Multitasking in tumor progression: signaling functions of cell adhesion molecules. Ann. N. Y. Acad. Sci. 1014, 58–66.

Cavey, M., Lecuit, T., 2009. Molecular bases of cell–cell junctions stability and dynamics. Cold Spring Harb. Perspect. Biol. 1, a002998.

Cooper, J.A., Sept, D., 2008. New insights into mechanism and regulation of actin capping protein. Int. Rev. Cell Mol. Biol. 267, 183–206.

Delalle, I., Pfleger, C.M., Buff, E., Lueras, P., Hariharan, I.K., 2005. Mutations in the *Drosophila* orthologs of the F-actin capping protein alpha- and beta-subunits cause actin accumulation and subsequent retinal degeneration. Genetics 171, 1757–1765.

Desprat, N., Supatto, W., Pouille, P.A., Beaurepaire, E., Farge, E., 2008. Tissue deformation modulates twist expression to determine anterior midgut differentiation in *Drosophila* embryos. Dev. Cell 15, 470–477.

Dow, L.E., Humbert, P.O., 2007. Polarity regulators and the control of epithelial architecture, cell migration, and tumorigenesis. Int. Rev. Cytol. 262, 253–302.

Fan, Y., Bergmann, A., 2008. Apoptosis-induced compensatory proliferation. The Cell is dead. Long live the Cell! Trends Cell Biol. 18, 467–473.

Fernandez, B.G., Gaspar, P., Bras-Pereira, C., Jezowska, B., Rebelo, S.R., Janody, F., 2011. Actin-capping protein and the Hippo pathway regulate F-actin and tissue growth in *Drosophila*. Development 138, 2337–2346.

Frame, M.C., 2004. Newest findings on the oldest oncogene; how activated src does it. J. Cell Sci. 117, 989–998.

Gates, J., Nowotarski, S.H., Yin, H., Mahaffey, J.P., Bridges, T., Herrera, C., Homem, C.C., Janody, F., Montell, D.J., Peifer, M., 2009. Enabled and capping protein play important roles in shaping cell behavior during *Drosophila* oogenesis. Dev. Biol. 333, 90–107.

Genevet, A., Polesello, C., Blight, K., Robertson, F., Collinson, L.M., Pichaud, F., Tapon, N., 2009. The Hippo pathway regulates apical-domain size independently of its growth-control function. J. Cell Sci. 122, 2360–2370.

Giannone, G., Sheetz, M.P., 2006. Substrate rigidity and force define form through tyrosine phosphatase and kinase pathways. Trends Cell Biol. 16, 213–223.

Gottardi, C.J., Wong, E., Gumbiner, B.M., 2001. E-cadherin suppresses cellular transformation by inhibiting beta-catenin signaling in an adhesion-independent manner. J. Cell Biol. 153, 1049–1060.

Goyal, L., McCall, K., Agapite, J., Hartwieg, E., Steller, H., 2000. Induction of apoptosis by *Drosophila* reaper, hid and grim through inhibition of IAP function. EMBO J. 19, 589–597.

Hariharan, I.K., Bilder, D., 2006. Regulation of imaginal disc growth by tumor-suppressor genes in *Drosophila*. Annu. Rev. Genet. 40, 335–361.

Hay, B.A., Wolff, T., Rubin, G.M., 1994. Expression of baculovirus P35 prevents cell death in *Drosophila*. Development 120, 2121–2129.

Hermiston, M.L., Wong, M.H., Gordon, J.I., 1996. Forced expression of E-cadherin in the mouse intestinal epithelium slows cell migration and provides evidence for nonautonomous regulation of cell fate in a self-renewing system. Genes Dev. 10, 985–996.

Igaki, T., 2009. Correcting developmental errors by apoptosis: lessons from *Drosophila* JNK signaling. Apoptosis 14, 1021–1028.

Igaki, T., Pagliarini, R.A., Xu, T., 2006. Loss of cell polarity drives tumor growth and invasion through JNK activation in *Drosophila*. Curr. Biol. 16, 1139–1146.

Jafar-Nejad, H., Tien, A.C., Acar, M., Bellen, H.J., 2006. Senseless and Daughterless confer neuronal identity to epithelial cells in the *Drosophila* wing margin. Development 133, 1683–1692.

Jaiswal, M., Agrawal, N., Sinha, P., 2006. Fat and Wingless signaling oppositely regulate epithelial cell–cell adhesion and distal wing development in *Drosophila*. Development 133, 925–935.

Jamora, C., Fuchs, E., 2002. Intercellular adhesion, signalling and the cytoskeleton. Nat. Cell Biol. 4, E101–E108.

Janody, F., Treisman, J.E., 2006. Actin capping protein alpha maintains vestigial-expressing cells within the *Drosophila* wing disc epithelium. Development 133, 3349–3357.

Jeanes, A., Gottardi, C.J., Yap, A.S., 2008. Cadherins and cancer: how does cadherin dysfunction promote tumor progression? Oncogene 27, 6920–6929.

Karim, F.D., Rubin, G.M., 1998. Ectopic expression of activated Ras1 induces hyperplastic growth and increased cell death in *Drosophila* imaginal tissues. Development 125, 1–9.

Kim, J.Y., Lee, Y.G., Kim, M.Y., Byeon, S.E., Rhee, M.H., Park, J., Katz, D.R., Chain, B.M., Cho, J.Y., 2009. Src-mediated regulation of inflammatory responses by actin polymerization. Biochem. Pharmacol. 79, 431–443.

Klein, T., Arias, A.M., 1998. Different spatial and temporal interactions between Notch, wingless, and vestigial specify proximal and distal pattern elements of the wing in *Drosophila*. Dev. Biol. 194, 196–212.

Kuranaga, E., Kanuka, H., Igaki, T., Sawamoto, K., Ichijo, H., Okano, H., Miura, M., 2002. Reaper-mediated inhibition of DIAP1-induced DTRAF1 degradation results in activation of JNK in *Drosophila*. Nat. Cell Biol. 4, 705–710.

Kurant, E., Pai, C.Y., Sharf, R., Halachmi, N., Sun, Y.H., Salzberg, A., 1998. *Dorsotonals/homothorax*, the *Drosophila* homologue of *meis1*, interacts with *extradenticle* in patterning of the embryonic PNS. Development 125, 1037–1048.

Lee, J.D., Treisman, J.E., 2001. Sightless has homology to transmembrane acyltransferases and is required to generate active Hedgehog protein. Curr. Biol. 11, 1147–1152.

Leong, G.R., Goulding, K.R., Amin, N., Richardson, H.E., Brumby, A.M., 2009. Scribble mutants promote aPKC and JNK-dependent epithelial neoplasia independently of Crumbs. BMC Biol. 7, 62.

Maitra, S., Kulikauskas, R.M., Gavilan, H., Fehon, R.G., 2006. The tumor suppressors Merlin and Expanded function cooperatively to modulate receptor endocytosis and signaling. Curr. Biol. 16, 702–709.

Martin-Blanco, E., Gampel, A., Ring, J., Virdee, K., Kirov, N., Tolkovsky, A.M., Martinez-Arias, A., 1998. Puckered encodes a phosphatase that mediates a feedback loop regulating JNK activity during dorsal closure in *Drosophila*. Genes Dev. 12, 557–570.

McEwen, D.G., Peifer, M., 2005. Puckered, a *Drosophila* MAPK phosphatase, ensures cell viability by antagonizing JNK-induced apoptosis. Development 132, 3935–3946.

Minn, A.J., Gupta, G.P., Siegel, P.M., Bos, P.D., Shu, W., Giri, D.D., Viale, A., Olshen, A.B., Gerald, W.L., Massague, J., 2005. Genes that mediate breast cancer metastasis to lung. Nature 436, 518–524.

Neumann, C.J., Cohen, S.M., 1997. Long-range action of Wingless organizes the dorsal–ventral axis of the *Drosophila* wing. Development 124, 871–880.

Nicolai, M., Lasbleiz, C., Dura, J.M., 2003. Gain-of-function screen identifies a role of the Src64 oncogene in *Drosophila* mushroom body development. J. Neurobiol. 57, 291–302.

Nienhaus, U., Aegerter-Wilmsen, T., Aegerter, C.M., 2009. Determination of mechanical stress distribution in *Drosophila* wing discs using photoelasticity. Mech. Dev. 126, 942–949.

Nolo, R., Abbott, L.A., Bellen, H.J., 2000. Senseless, a Zn finger transcription factor, is necessary and sufficient for sensory organ development in *Drosophila*. Cell 102, 349–362.

Ollmann, M., Young, L.M., Di Como, C.J., Karim, F., Belvin, M., Robertson, S., Whittaker, K., Demsky, M., Fisher, W.W., Buchman, A., Duyk, G., Friedman, L., Prives, C., Kopczynski, C., 2000. *Drosophila* p53 is a structural and functional homolog of the tumor suppressor p53. Cell 101, 91–101.

Orsulic, S., Huber, O., Aberle, H., Arnold, S., Kemler, R., 1999. E-cadherin binding prevents beta-catenin nuclear localization and beta-catenin/LEF-1-mediated transactivation. J. Cell Sci. 112 (Pt 8), 1237–1245.

Pagliarini, R.A., Xu, T., 2003. A genetic screen in *Drosophila* for metastatic behavior. Science 302, 1227–1231.

Panganiban, G., Sebring, A., Nagy, L., Carroll, S., 1995. The development of crustacean limbs and the evolution of arthropods. Science 270, 1363–1366.

Peifer, M., Pai, L.M., Casey, M., 1994. Phosphorylation of the *Drosophila* adherens junction protein Armadillo: roles for wingless signal and zeste-white 3 kinase. Dev. Biol. 166, 543–556.

Perez-Garijo, A., Shlevkov, E., Morata, G., 2009. The role of Dpp and Wg in compensatory proliferation and in the formation of hyperplastic overgrowths caused by apoptotic cells in the *Drosophila* wing disc. Development 136, 1169–1177.

Prober, D.A., Edgar, B.A., 2000. Ras1 promotes cellular growth in the *Drosophila* wing. Cell 100, 435–446.

Prober, D.A., Edgar, B.A., 2002. Interactions between Ras1, dMyc, and dPI3K signaling in the developing *Drosophila* wing. Genes Dev. 16, 2286–2299.

Ryoo, H.D., Bergmann, A., Gonen, H., Ciechanover, A., Steller, H., 2002. Regulation of *Drosophila* IAP1 degradation and apoptosis by reaper and ubcD1. Nat. Cell Biol. 4, 432–438.

Ryoo, H.D., Gorenc, T., Steller, H., 2004. Apoptotic cells can induce compensatory cell proliferation through the JNK and the Wingless signaling pathways. Dev. Cell 7, 491–501.

Sanson, B., White, P., Vincent, J.P., 1996. Uncoupling cadherin-based adhesion from wingless signalling in *Drosophila*. Nature 383, 627–630.

Sansores-Garcia, L., Bossuyt, W., Wada, K.I., Yonemura, S., Tao, C., Sasaki, H., Halder, G., 2011. Modulating F-actin organization induces organ growth by affecting the Hippo pathway. EMBO J. 30, 2325–2335.

Shindo, M., Wada, H., Kaido, M., Tateno, M., Aigaki, T., Tsuda, L., Hayashi, S., 2008. Dual function of Src in the maintenance of adherens junctions during tracheal epithelial morphogenesis. Development 135, 1355–1364.

Spradling, A.C., Stern, D., Beaton, A., Rhem, E.J., Laverty, T., Mozden, N., Misra, S., Rubin, G.M., 1999. The Berkeley Drosophila Genome Project gene disruption project: single P-element insertions mutating 25% of vital *Drosophila* genes. Genetics 153, 135–177.

Stockinger, A., Eger, A., Wolf, J., Beug, H., Foisner, R., 2001. E-cadherin regulates cell growth by modulating proliferation-dependent beta-catenin transcriptional activity. J. Cell Biol. 154, 1185–1196.

Sun, G., Irvine, K.D., 2011. Regulation of Hippo signaling by Jun kinase signaling during compensatory cell proliferation and regeneration, and in neoplastic tumors. Dev. Biol. 350, 139–151.

Tang, C.Y., Sun, Y.H., 2002. Use of mini-white as a reporter gene to screen for GAL4 insertions with spatially restricted expression pattern in the developing eye in *Drosophila*. Genesis 34, 39–45.

Tepass, U., Gruszynski-DeFeo, E., Haag, T.A., Omatyar, L., Torok, T., Hartenstein, V., 1996. Shotgun encodes *Drosophila* E-cadherin and is preferentially required during cell rearrangement in the neurectoderm and other morphogenetically active epithelia. Genes Dev. 10, 672–685.

Uemura, T., Oda, H., Kraut, R., Hayashi, S., Kotaoka, Y., Takeichi, M., 1996. Zygotic *Drosophila* E-cadherin expression is required for processes of dynamic epithelial cell rearrangement in the *Drosophila* embryo. Genes Dev. 10, 659–671.

Uhlirova, M., Bohmann, D., 2006. JNK- and Fos-regulated Mmp1 expression cooperates with Ras to induce invasive tumors in *Drosophila*. EMBO J. 25, 5294–5304.

Uhlirova, M., Jasper, H., Bohmann, D., 2005. Non-cell-autonomous induction of tissue overgrowth by JNK/Ras cooperation in a *Drosophila* tumor model. Proc. Natl. Acad. Sci. U. S. A. 102, 13123–13128.

van Roy, F., Berx, G., 2008. The cell–cell adhesion molecule E-cadherin. Cell. Mol. Life Sci. 65, 3756–3788.

Please cite this article as: Jezowska, B., et al., A dual function of *Drosophila* capping protein on DE-cadherin maintains epithelial integrity and prevents JNK-mediated apoptosis, Dev. Biol. (2011), doi:10.1016/j.ydbio.2011.09.016

Vidal, M., Larson, D.E., Cagan, R.L., 2006. Csk-deficient boundary cells are eliminated from normal *Drosophila* epithelia by exclusion, migration, and apoptosis. Dev. Cell 10, 33–44.
Vidal, M., Warner, S., Read, R., Cagan, R.L., 2007. Differing Src signaling levels have distinct outcomes in *Drosophila*. Cancer Res. 67, 10278–10285.
Wang, S.L., Hawkins, C.J., Yoo, S.J., Muller, H.A., Hay, B.A., 1999. The *Drosophila* caspase inhibitor DIAP1 is essential for cell survival and is negatively regulated by HID. Cell 98, 453–463.
Widmann, T.J., Dahmann, C., 2009. Wingless signaling and the control of cell shape in *Drosophila* wing imaginal discs. Dev. Biol. 334, 161–173.
Winder, S.J., Ayscough, K.R., 2005. Actin-binding proteins. J. Cell Sci. 118, 651–654.
Wodarz, A., Hinz, U., Engelbert, M., Knust, E., 1995. Expression of *crumbs* confers apical character on plasma membrane domains of ectodermal epithelia of *Drosophila*. Cell 82, 67–76.
Wu, M., Pastor-Pareja, J.C., Xu, T., 2010. Interaction between Ras(V12) and scribbled clones induces tumour growth and invasion. Nature 463, 545–548.
Yoo, S.J., Huh, J.R., Muro, I., Yu, H., Wang, L., Wang, S.L., Feldman, R.M., Clem, R.J., Muller, H.A., Hay, B.A., 2002. Hid, Rpr and Grim negatively regulate DIAP1 levels through distinct mechanisms. Nat. Cell Biol. 4, 416–424.
Zecca, M., Basler, K., Struhl, G., 1996. Direct and long-range action of a wingless morphogen gradient. Cell 87, 833–844.

Please cite this article as: Jezowska, B., et al., A dual function of *Drosophila* capping protein on DE-cadherin maintains epithelial integrity and prevents JNK-mediated apoptosis, Dev. Biol. (2011), doi:10.1016/j.ydbio.2011.09.016